

15

MAR 23 1998

## SANDIA REPORT

SAND98-0306 • UC-1302  
Unlimited Release  
Printed February 1998

RECEIVED  
MAR 27 1998  
OSTI

# Boundary Element Method Applied to a Gas-Fired Pin-Fin-Enhanced Heat Pipe

DISTRIBUTION OF THIS DOCUMENT IS UNLIMITED

Charles E. Andraka, Gerald A. Knorovsky, Celeste A. Drewien

Prepared by  
Sandia National Laboratories  
Albuquerque, New Mexico 87185 and Livermore, California 94550

Sandia is a multiprogram laboratory operated by Sandia Corporation,  
a Lockheed Martin Company, for the United States Department of  
Energy under Contract DE-AC04-94AL85000.

Approved for public release; further dissemination unlimited.

DTIC QUALITY INSPECTED 3

MASTER



Sandia National Laboratories

19980507 014

Issued by Sandia National Laboratories, operated for the United States Department of Energy by Sandia Corporation.

**NOTICE:** This report was prepared as an account of work sponsored by an agency of the United States Government. Neither the United States Government nor any agency thereof, nor any of their employees, nor any of their contractors, subcontractors, or their employees, makes any warranty, express or implied, or assumes any legal liability or responsibility for the accuracy, completeness, or usefulness of any information, apparatus, product, or process disclosed, or represents that its use would not infringe privately owned rights. Reference herein to any specific commercial product, process, or service by trade name, trademark, manufacturer, or otherwise, does not necessarily constitute or imply its endorsement, recommendation, or favoring by the United States Government, any agency thereof, or any of their contractors or subcontractors. The views and opinions expressed herein do not necessarily state or reflect those of the United States Government, any agency thereof, or any of their contractors.

Printed in the United States of America. This report has been reproduced directly from the best available copy.

Available to DOE and DOE contractors from  
Office of Scientific and Technical Information  
P.O. Box 62  
Oak Ridge, TN 37831

Prices available from (615) 576-8401, FTS 626-8401

Available to the public from  
National Technical Information Service  
U.S. Department of Commerce  
5285 Port Royal Rd  
Springfield, VA 22161

NTIS price codes  
Printed copy: A05  
Microfiche copy: A01



## **Boundary Element Method Applied to a Gas-Fired Pin-Fin-Enhanced Heat Pipe**

**Charles E. Andraka**  
**Solar Thermal Technology**

**Gerald A. Knorovsky**  
**Materials Joining Department**

**Celeste A. Drewien**  
**Microstructural Analysis**

**Sandia National Laboratories**  
**P.O. Box 5800**  
**Albuquerque NM 87185-0703**

### **ABSTRACT**

The thermal conduction of a portion of an enhanced-surface heat exchanger for a gas-fired heat pipe solar receiver was modeled using the boundary element and finite element methods (BEM and FEM) to determine the effect of weld fillet size on performance of a stud-welded pin fin. A process that could be utilized by others for designing the surface mesh on an object of interest, performing a conversion from the mesh into the input format utilized by the BEM code, obtaining output on the surface of the object, and displaying visual results was developed. It was determined that the weld fillet on the pin fin significantly enhanced the heat performance, improving the operating margin of the heat exchanger.

The performance of the BEM program on the pin fin was measured (as computational time) and used as a performance comparison with the FEM model. Given similar surface element densities, the BEM method took longer to get a solution than the FEM method. The FEM method creates a sparse matrix that scales in storage and computation as the number of nodes (N), whereas the BEM method scales as  $N^2$  in storage and  $N^3$  in computation.

## TABLE OF CONTENTS

<b>INTRODUCTION.....</b>	<b>1</b>
<b>BACKGROUND.....</b>	<b>1</b>
THE HEAT EXCHANGER AND PIN FIN .....	1
THE BOUNDARY ELEMENT METHOD .....	5
<b>PURPOSE.....</b>	<b>7</b>
<b>APPROACH.....</b>	<b>7</b>
PROJECT PLAN.....	7
BEM 3D STEADY STATE CODE.....	8
CODE MODIFICATIONS .....	10
TIMING TESTS.....	10
MESH DESCRIPTION.....	11
CUBE TRIAL RUNS.....	11
MESH GENERATION.....	12
MESH CONVERSION.....	13
DATA VISUALIZATION.....	15
PIN FIN ANALYSIS .....	15
FINITE ELEMENT METHOD APPLIED TO PIN FIN.....	16
<b>RESULTS .....</b>	<b>17</b>
CUBE RESULTS .....	17
PIN FIN BEM RESULTS.....	19
PIN FIN FEM RESULTS .....	23
TIMING RESULTS .....	28
<b>SUMMARY/CONCLUSIONS .....</b>	<b>31</b>
<b>ACKNOWLEDGMENTS .....</b>	<b>32</b>
<b>REFERENCES.....</b>	<b>33</b>
<b>APPENDIX A. NPOT3D BEM CODE.....</b>	<b>34</b>
<b>APPENDIX B. FEM SESSION FILES .....</b>	<b>61</b>
<b>APPENDIX C. CONVERSION CODE.....</b>	<b>65</b>
<b>DISTRIBUTION.....</b>	<b>74</b>

## List of Figures

<i>Figure 1--The Advanco system holds the gross system conversion efficiency record of 30.6%. About 75kW, sunlight is concentrated by the 11-m diameter dish onto the receiver. A Stirling engine converts the heat flux into grid-ready electricity. The Advanco system, tested in the early 80's, does not incorporate a heat pipe.....</i>	2
<i>Figure 2--This diagram shows a typical solar-only heat-pipe receiver and Stirling engine. Concentrated sunlight impinges on the spherical absorber, which is cooled by evaporating sodium. The sodium condenses on the engine heater tubes, releasing latent heat. The gas-fired portion will be added as a cylinder separating the absorber dome from the rear support dome. ....</i>	3
<i>Figure 3--The schematic shows the evaporator end of the sub-scale gas-fired heat-pipe receiver. Preheated air-fuel enters the system through the left plenum, and burns at the matrix burner. The hot gases are then directed through the pin-fin array by high-temperature insulation. The exhaust gases are collected by another plenum and routed to the recuperator. Liquid sodium evaporates from the capillary wick, cooling the heated wall.....</i>	3
<i>Figure 4--This photo shows about 1600 pins welded to a 76.2mm (3")-diameter heat pipe. This sub-scale device will be used to validate the various models and design codes before a full-scale device is fabricated.....</i>	4
<i>Figure 5--This sample weld cross-section clearly shows the conical fillet formed by the stud-welding process. We assumed that the material thermal properties are unchanged in the melt region of the weld. The weld is autogenous, i.e. no filler metal was added. ....</i>	5
<i>Figure 6--Local node numbering for a nine node continuous quadrilateral element.....</i>	11
<i>Figure 7a and b—Flux out bottom surface of cube (expressed as temperature gradient, °C/mm) and temperature distribution across cube (°C) for cube meshed with 64 elements per side. ....</i>	18
<i>Figure 8--Output of results from collocation points in the center of a cube and moving towards the top surface of the cube, which was meshed with one element per side.....</i>	19
<i>Figure 9a. --BEM meshes of the 2X filleted pin fin model.....</i>	20
<i>Figure 10 a and b—Temperature and gradient distribution for the straight pin fin (IX). ....</i>	22
<i>Figure 11--a.) Temperature distribution for the 2X filleted pin fin (°C). b.) Gradient distribution for the 2X filleted pin fin (°C/mm). ....</i>	22
<i>Figure 12--Variation in BEM-calculated heat flux distribution for filleted and straight pin fins with respect to mesh density.....</i>	24
<i>Figure 13--a.) IX FEM and 1/2X FEM mesh (20 nodes/element &amp; 8 nodes/element, respectively) and b.) 1/4X FEM mesh.....</i>	25
<i>Figure 14--Heat flux in z direction (W/mm<sup>2</sup>) and Temperature(°C) distributions calculated by FEM for a.) IX, b.) 1/2X, and c.) 1/4X meshes. ....</i>	27
<i>Figure 15--Heat flux in z direction (W/mm<sup>2</sup>) along bottom diagonal of pin fin, calculated by FEM for IX, 1/2X, and 1/4X meshes. ....</i>	28
<i>Figure 16—BEM Timing results for total time and portions of the code. Time is in seconds. ....</i>	30
<i>Figure 17--Total FEM calculation time vs number of nodes in model. ....</i>	31

### *List of Tables*

<i>Table 1--Boundary Conditions for Pin Fin.....</i>	17
<i>Table 2--Peak temperature and flux with mesh density. The results are for the BEM model except as noted. ....</i>	24
<i>Table 3--Comparison of BEM and TEM bottom surface nodal density (number of bottom surface nodes in models)28</i>	
<i>Table 4--Comparison of BEM run times with differing levels of code optimization on the RS6000 computer.....</i>	29
<i>Table 5--Output from timing tests for differing number of nodes. Results were obtained using an IBM RS6000 with an optimizer level of 2 and requesting uninterrupted use of one processor. ....</i>	29

## Introduction

In this project, we model the thermal conduction of a portion of an enhanced-surface heat exchanger for a gas-fired heat pipe solar receiver. The surface enhancement is accomplished by an array of pin fins on the gas-fired side of the heat exchanger. In prior work, the heat exchanger assembly was modeled in Fluent UNS, a commercial computational fluid dynamics code[1], to determine the hot gas flow field over the pin fin array. The Fluent modeling indicated high local thermal flux at several pin rows. The results of the Fluent modeling (gas temperature and convection coefficient) were used in a finite element program (COSMOS/M, v1.75)[2] to determine the stresses and heat transfer at the critical pin fin in much greater detail. The calculated thermal flux and peak pin-tip temperatures were sufficiently high to cause concern for the unit's service life.

Since then, weld procedures have been developed and refined in order to get consistent automated welds of the pin fins to the wall material. The resulting weld has a conical fillet around the base of the pin, which was not included in the original modeling. The purpose of the current work is to determine the relative effect of this fillet on the heat transfer characteristics of the pin. In particular, we are interested in the effect on the peak pin temperature (materials limitations) and on the local flux distribution into the heat pipe wick (wick limitation).

Since all of the areas of interest lie on the outer surfaces, or boundaries, of the pin structure, we do not need a full-field solution such as given by finite element methods (FEM). Therefore, this problem would seem to be natural match for the boundary element method (BEM).

In solving this heat transfer problem, we develop a process that could be utilized by others for designing the surface mesh on an object of interest, performing a conversion from the mesh into the input format utilized by the BEM code [3], obtaining output on the surface of the object, and displaying visual results. The process was first tried on a simple cube with known analytic solution. Once the process was established, it was applied to the pin fins. The performance of the BEM program on the pin fin was measured (as computational time) and used as a performance comparison with the FEM model. The approach and process are presented here, and can be used for application to similar problems.

## Background

### *The Heat Exchanger and Pin Fin*

The heat pipe receiver is a component of a solar thermal heat receiver for a dish-Stirling electric generation system. In solar-only operation, a heat pipe acts as a “heat transformer,” accepting the non-uniform concentrated sunlight from a parabolic dish and transferring the heat uniformly and isothermally to a Stirling engine (Figure 1)[4]. The inside surface of the heat pipe absorber is covered with a porous structure saturated with liquid sodium. The heat pipe enclosure is evacuated. The concentrated solar flux is absorbed through the absorber surface, evaporating

the sodium, which limits the absorber surface temperature. The vapor generated flows to the heater heads, where it condenses and its latent heat is transferred isothermally to the Stirling engine (Figure 2). The condensed liquid is returned to the wick structure with the aid of gravity. The porous structure re-distributes the condensed sodium by capillary pumping. The entire process is similar to a double boiler used for cooking.

There is a need by some potential customers to operate without regard to local weather conditions. Therefore, a "hybrid" system that can operate in solar and/or natural-gas-fired modes is being developed. In this configuration, a spherical absorber is used for absorbing concentrated solar energy, and a cylindrical sidewall is used to absorb heat from burning natural gas. Figure 3 schematically shows a gas-fired (only) prototype heat pipe.

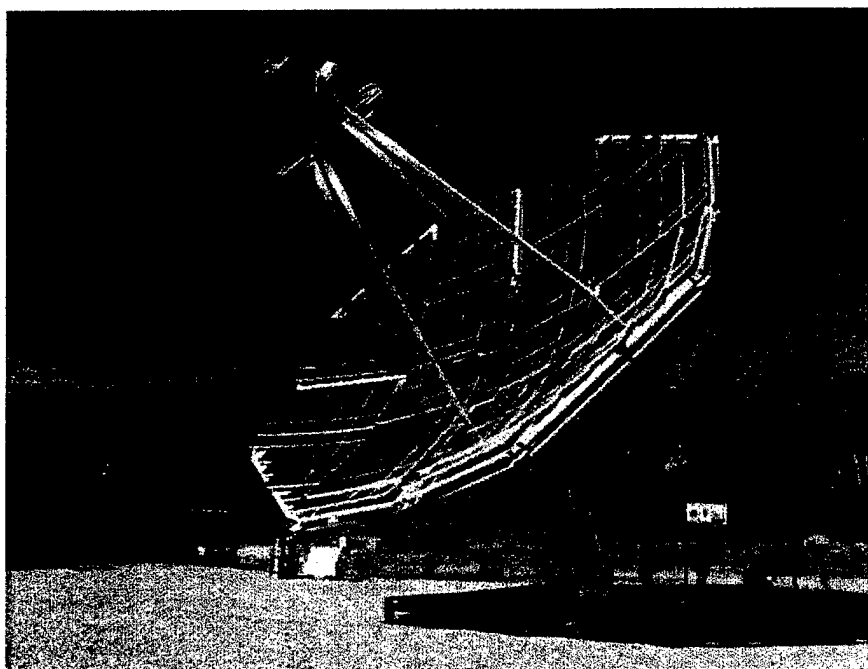


*Figure 1--The Advanco system holds the gross system conversion efficiency record of 30.6%. The 11-m diameter dish concentrates about 75kW, sunlight is onto the receiver. A Stirling engine converts the heat flux into grid-ready electricity. The Advanco system, tested in the early 80's, does not incorporate a heat pipe.*

Heat transfer from the gas burner to the heat pipe requires a large area. However, the size of the heat exchanger must be minimized because the materials (Haynes alloy 230) are expensive and the wicking limitations of the heat pipe capillary structure dictate maximum sodium pumping distances (When pressure drops caused by gravity or flow through the wick exceed the capillary pressure of the wick structure, distribution of the sodium ceases and the heat pipe fails).

In order to efficiently collect the heat from the gas in a small area, the heat transfer surface had to be enhanced. Cost and stress issues led us to a stud-welded pin-fin arrangement. The pins are 6.35 mm tall by 3.18 mm diameter. The wall thickness is 0.889 mm. The aspect ratio was determined to some extent by the automated stud welder limitations. The envisioned full-scale

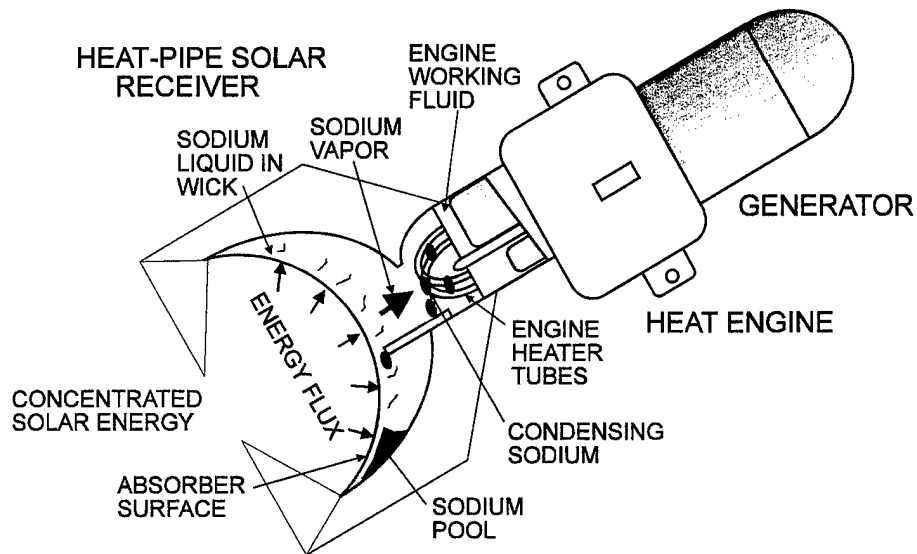


Figure 2--This diagram shows a typical solar-only heat-pipe receiver and Stirling engine. Concentrated sunlight impinges on the spherical absorber, which is cooled by evaporating sodium. The sodium condenses on the engine heater tubes, releasing latent heat. The gas-fired portion will be added as a cylinder separating the absorber dome from the rear support dome.

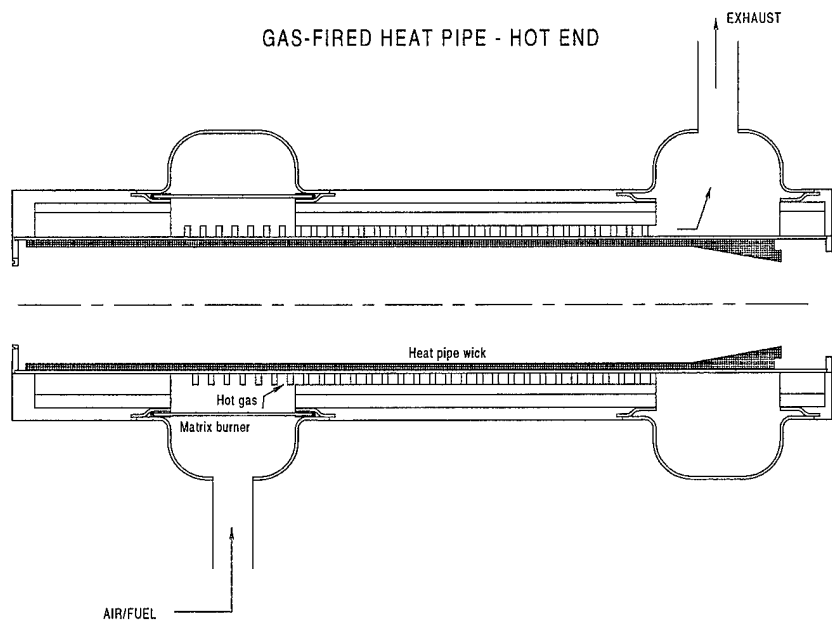
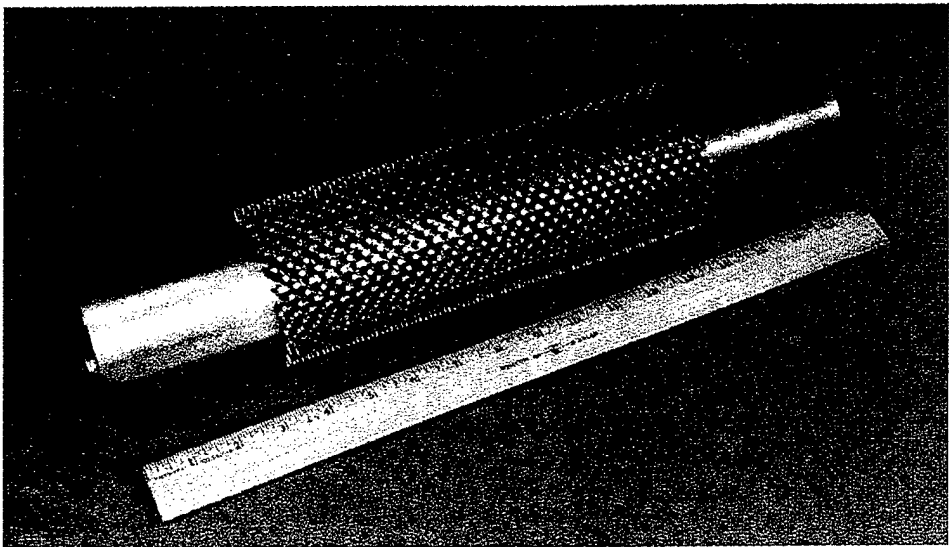


Figure 3--The schematic shows the evaporator end of the sub-scale gas-fired heat-pipe receiver. Preheated air-fuel enters the system through the left plenum, and burns at the matrix burner. The hot gases are then directed through the pin-fin array by high-temperature insulation. The exhaust gases are collected by another plenum and routed to the recuperator. Liquid sodium evaporates from the capillary wick, cooling the heated wall.



*Figure 4--This photo shows about 1600 pins welded to a 76.2mm (3")-diameter heat pipe. This sub-scale device will be used to validate the various models and design codes before a full-scale device is fabricated.*

10,000 pins to transfer  $75\text{kW}_t$  (see Figure 4). The gas enters the system at around  $1700^\circ\text{C}$ , and the heat pipe operates at  $750^\circ\text{C}$  internal sodium vapor temperature. The addition of heat to such a hot surface presents many challenges, including recuperation (to recover heat from the  $800^\circ\text{C}$  exhaust gasses) preignition (potentially caused by the high pre-heat), low thermal driving potential (hot gases heating an already-hot surface), high thermal stresses, and materials life issues.

The first several inches of the heat transfer region face the matrix burner, and the flow of the burning gas is radially inward. The gas is then directed axially through the remainder of the pin-fin array, and then is collected by the exhaust plenum and passed to the recuperator. Fluent UNS modeling of the gas flow and gas-side heat transfer indicates that the first row of pins, after the flow is diverted from radial to longitudinal, is the most "effective" row with the highest combined convection coefficient and gas temperature, thereby resulting in the highest peak flux through the heat pipe wall.

The resulting flux distribution into the wick, as calculated by Fluent UNS, was on too coarse a mesh to evaluate the wick behavior. Using a finite element package (COSMOS/M), a single pin was modeled to examine the local flux distribution, the pin tip temperature, and the stresses at the pin root. The flux distribution was then used in a wick modeling routine to evaluate the wick performance. The resulting liquid pressure drops in the wick limited the throughput power capabilities of the heat pipe below acceptable levels. In addition, the estimated peak temperature of the pin fin tips approached the maximum working temperature of the Haynes-230 alloy.

When preliminary manufacturing studies and tests on the stud welds were completed, the preferred weld had a significant fillet at the pin/wall interface (Figure 5). This fillet (consisting of approximately 1.5 mm of the total pin height with a base diameter of ~4.5 mm) has the potential to significantly spread the flux presented to the wick. In this effort, the extent of this spreading

and the added benefit of possible reduced pin tip temperatures will be investigated. Reduced pin temperatures may also improve the pin effectiveness, which can be seen in the total heat transfer through a given pin.

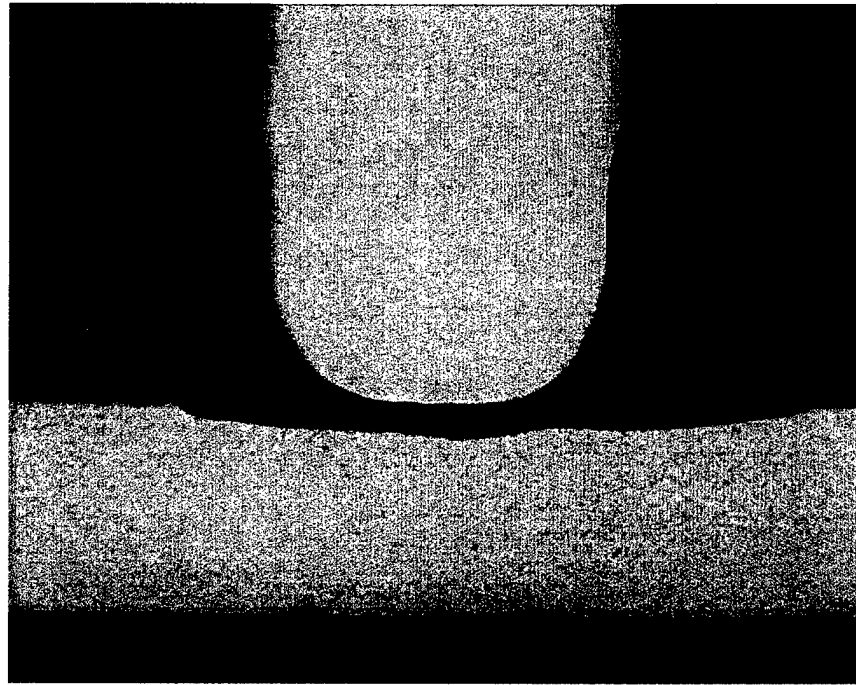


*Figure 5--This sample weld cross-section clearly shows the conical fillet formed by the stud-welding process. We assumed that the material thermal properties are unchanged in the melt region of the weld. The weld is autogenous, i.e. no filler metal was added.*

### ***The Boundary Element Method***

This section provides a brief introduction to the modeling method used in this investigation.

The boundary element method for solving partial differential equations is applicable to a wide class of linear elliptic boundary value problems, allowing reduction in the dimensionality of the problem. Spatial discretization of the domain boundary is the only requirement for a steady state problem, however the method can be extended to transient problems where temporal discretization would be required also. Boundary spatial discretization could significantly reduce the workload in solving a problem over that of a finite element method (FEM). The method has been successfully applied to a variety of problems [5].

The BEM relies upon some mathematical legerdemain (the Green-Gauss theorem) to reduce a three-dimensional (3D) volume domain partial differential equation problem to a two-dimensional (2D) surface domain one. This offers some advantages as well as disadvantages. In general, computational requirements scale with the size of the problem being investigated; if one can reduce a problem from the number of nodes/elements required to fill volume, to the number

required to cover the surface area, there is a strong likelihood that the computation will run faster. In particular, claimed advantages for the BEM method over more conventional volume domain methods include:

- i.) As already noted, the dimensionality of the problem is reduced by one, e.g. from a volume to a surface; this simplifies the structure of vectors and matrices needed to represent the elements being computed, and simplifies the programming and storage requirements in like fashion. Without tricks, a 3-D array would require three nested do loops to be accessed or modified, while a 2-D array would only require two. In reality, this oversimplifies the problem; however, even if comparable depths of nested loops are employed, the number of elements may be considerably smaller for the BEM than for the FEM. The resulting array is fully dense and solved with a direct solver. However, the array is smaller than an FEM array with a similar surface-density of elements.
- ii.) The system of algebraic equations which are solved are generally well-conditioned, showing diagonal dominance.
- iii.) The method can handle regions that are infinite in extent.
- iv.) The meshes (being representative of surfaces) are generally simpler to generate.
- v.) Problems involving surfaces or surface discontinuities, interfaces and moving boundaries may be handled. The prototypical example is in calculations of stress in regions of geometrical discontinuity (notches and cracks).
- vi.) Generation of a full field solution is not necessary; in other words, to study a small region of a larger problem, the entire solution does not have to be generated. A surface solution is generated, then additional collocation point solutions are generated in internal areas of interest..

This last ‘advantage’ may not be one if the full-field solution is of interest.

Some of the disadvantages of BEM are:

- i.) The individual equations of the system of equations have many terms, and matrix decomposition is more complex and slower than for FEM’s sparse arrays. The matrix is generally full.
- ii.) The method is best suited for problems where a fundamental solution (or an approximation) to the adjoint operator is available for the governing differential equation, limiting applicability to certain problems. The adjoint operator is the transpose of the cofactor matrix; its product with the inverse of the determinant gives the inverse of the matrix.

The desired outputs of the pin-fin heat flow analysis are the maximum pin temperature at its adiabatic top surface, and the heat flux distribution out the bottom surface of the shell to which it is welded. While the thermal analysis by FEM methods is tractable for a single pin in isolation, if multiple pins acting in concert were to be analyzed, it was thought that the problem might become intractable very quickly. These points suggested that the BEM might be appropriate alternative for the pin fin analysis.

Two implementations of the BEM method are typically employed. The direct method employs unknowns that are actual physical variables (this is the method used herein). In the

indirect method, the unknowns are represented by a density function that is distributed over the boundary; this does not lend itself to physical interpretation. However, once the density function has been determined completely, physical variables can be deduced.

This latter method leads to the last disadvantage of the BEM approach; it can be difficult to understand! Unlike the Finite Difference (FD) and FEM approaches, which are basically straightforward, this method relies upon some abstract mathematical foundations. Thus, qualitatively comparing the algorithms used to set up the matrix from which solutions are calculated, the FD approach is easy, the FEM approach is moderately easy, and the BEM is difficult. While using an already written code goes a long way to alleviate this problem, when problems are encountered, as they inevitably will be, debugging becomes difficult. Thus, the approach here was to start small and simple as described below.

## Purpose

The goals of this investigation were to determine the following:

- What are the thermal flux and temperature distributions on the pin fin?
- How did the weld fillet influence the heat transfer in the pin fin (What is the effect of the weld geometry vs. the idealized cylindrical pin)?
- Is there any thermal performance gain realized by the fillet on the actual welded pin fin?
- Are there significant computational speed advantages for the BEM over the FEM approach?
- How do the BEM results compare with the FEM results?
- What level of mesh size could be used to obtain reasonable results for BEM vs FEM?  
What was the order of the calculation relative to the number of nodes in the mesh?

## Approach

### *Project Plan*

In order to apply the boundary element method to the pin fin problem, the following tasks had to be accomplished:

- i.) Obtain-BEM steady state code.
- ii.) Get code to run.
- iii.) Determine method to build mesh for pin fin. We knew that the original FEM mesh used in the stress analysis for the pin fin had about 10,000 nodes, so this had to be an automated method.
- iv.) Determine method to apply boundary conditions (BC's) to the meshed object.
- v.) Determine method to produce appropriate input file for the BEM code. The BEM program needed to have a particular data structure linking local and global representations of the nodes. It also needed to have data in a particular format.

- vi.) Determine method to extract data from code output files. The normal method is to use collocation nodes which are interior to the domain. Since we were looking on the surface, the results were calculated directly, but were not transparent without some further code modification.
- vii.) Determine method to plot data. Interpretation of large data structures is difficult without a suitable visualization tool. In the case of the heat flow problem, direct visualization of the temperatures and heat fluxes superimposed on the actual part is the most straightforward way.

### ***BEM 3D Steady State Code***

The boundary element code, npot3d.f, was developed by Marc Ingber [3], University of New Mexico. The code is written in Fortran77. For this investigation, it was run using an xlf compiler on the IBM RS6000 computer in addition to the comparison testing with the FEM model which was performed on a desktop computer. The code in its present form contains very little internal documentation, but two reports for input file format [6] and boundary element formulation and program description for the transient heat conduction problem[5] exist. A brief overview of the program (listing provided in Appendix A) follows.

The main program initializes variables, constants, and the input file name. All arrays are dimensioned. The input file and output files are opened. Then the subroutines QUADR, GEOM, MATVEC, DECOMP, SOLVE, and CALPHI are called before final data is output and the program ends.

Subroutine GEOM reads data from the input file:

#### **Titles**

whether the domain is interior or exterior

number of additional collocation points chosen outside of the domain

number of nodes

number of elements

node number

x, y, and z coordinates

boundary condition value and type

local node to global node

number of collocation points

x, y, and z coordinates of collocation points for obtaining an approximate solution.

Subroutine MATVEC collects and assembles vectors and matrix A. It sets up collocation points based upon the interior or exterior of the domain and then calls Subroutine INT4 to integrate the Green's integrals. On return the A matrix and B vector are filled in based upon whether temperature or flux or both were specified for the boundary condition. The A matrix is filled utilizing Ah1 and Ah2 vectors. The B vector is filled using B, Phi, Ah1, and Ah2 vectors.

Subroutine INT4 identifies coordinates based upon element type--triangular or quadrilateral. It calculates the distance of the surface collocation point to the surrounding local nodes, sets the value of "inode" based upon that distance relative to small (1e-6) and then calls subroutine RQINT for a quadrilateral element type. On return G1 and G1P values are available for calculation of the Ah1 and Ah2 vectors.

Subroutine RQINT is book keeping in nature. If the element type is continuous quadrilateral then subroutine RQINTC is called, otherwise RQINTD is called for the discontinuous quadrilateral element.

Subroutine RQINTC finds the longest diagonal of the element (H), then finds the distance from the surface collocation point to the center of the element (D). The severity is H/D. Thus, the smaller the distance D, the larger the severity value. If the severity value is less than 0.358, then the severity number is 1, otherwise subroutine DER9T is called. If DER9T is called, then a new distance is calculated based upon use of a smaller sub-spacing during quadrature. Effectively, the derivative times the coordinates are summed to find a new gauss point. The normal to the element surface (q) is found and converted to a unit normal vector (u) in subroutine UNORMAL. On return the dot product of u with the vector from the element center to the collocation point is performed to find the angle between the two vectors. A new severity number is calculated and a warning is sent if the severity number is greater than 9. DER9T is called again and gauss weighting is used for the distance determination. The surface normal and its unit vector are calculated and then subroutine FUNDS is called. On return from FUNDS, G1 and G1P vectors are formed before returning to INT4.

Subroutine DER9T is the derivative of the shape function for the 9 local node quadrilateral element.

Subroutine UNORMAL calculates the surface normal to the element (q) and its unit vector (u).

Subroutine DER9TD returns the derivative of the shape function for the discontinuous element.

Subroutine FUNDS calls the appropriate shape function routine based upon the element type. For the continuous quadrilateral, SH9T is shape function for the 9 node continuous quadrilateral element.

Subroutine DECOMP is a matrix decomposition routine using LU decomposition.

Subroutine SOLVE uses back substitution to solve the linear algebra equation. Here matrix A and vector B are used to find the solution vector.

Subroutine CALPHI calculates the approximate solution at the collocation points of interest to the program user. This routine was not utilized for this work because only answers on the

surface were of interest; the answers were either in the specified boundary condition vectors or easily obtained from the solution vector.

### **Code Modifications**

Some modifications to the npot3d.f code were performed to facilitate use on this project (see Appendix A). These modifications are summarized as follows:

- i.) Several "OPEN" statements were added in order to output particular data to separate files. Output of the solution vector and the boundary conditions were combined to form an output file called \*.plt, which contains columns of "Node", "Temperature", and "Flux". Another output file was created for the timing operations that were added to the program; this output file is \*.tim and contains readable lines of code with the time specified by the machine (here in seconds). The output file \*.out outputs "x", "y", and "z" coordinates along with "Temperature". This is the standard output file that would result from input of collocation points. This file may be useful to some users if collocation points are desired. Alternately, the slight difference in the \*.plt and \*.out files is based upon the ability to plot in 3 dimensions. The plotting routine employed in this effort was the COSMOS/M program that was used to generate the mesh; the surface was defined by the node number and visual output was easily obtained from the \*.plt file.
- ii.) A "READ" statement for keyboard entry of the name of the input file was added. This feature is optional and can easily be commented out: *root*, the filename without the extension is simply assigned the 'filename'. Note the filename has to be 8 characters long. For batch-mode timing tests with llssubmit (see next section), this name had to be entered prior to execution and these two lines had to be commented out of the code.
- iii.) Timing was added to the program in order to see the influence of mesh size on the time required by the various subroutines--MATVEC, GEOM, DECOMP/SOLVE, and CALPHI. The total time was also reported. Timing was performed using the mytime.f program[6].
- iv.) The pointers to the first element in an array were specified as "array(1)" in the dimension statements of the subroutines. The xlf compiler does not accept this notation and the "1" was changed to an "\*" in order to specify the pointer and not indicate an array size of 1.
- v.) Array dimensions were initially set to 600 for the matrix, forcing vector, and solution vector in addition to many other arrays that relied upon the number of elements. The array dimensions were changed to 4000 to accommodate the size of the input meshes used in this work.
- vi.) Comments were added to aid future users.

### **Timing Tests**

Timing tests were run using npot3d.f with mytime.f [7] on an IBM RS6000 computer. Originally, no optimizer level was specified and timing was performed without requesting uninterrupted use of one node of the machine. Next, the timing tests were rerun using the same files but requesting uninterrupted use of one node of an IBM SP1 computer (one node is identical

to the RS6000) through the llsubmit command. A command file (\*.cmd) was formulated in which the \*.in and \*.out were not designated because the npot3d.f code opens standard input (unit 5) and output (unit 6) during the execution. Timing was performed for the total run time and the subroutines GEOM, MATVEC, DECOMP/SOLVE, and CALPHI and writing to output files. Note that the time around both the DECOMP and SOLVE subroutines was combined into one interval. Some timing results were also supplied as standard output of the COSMOS/M FEM code.

### ***Mesh Description***

The BEM code requires 6-node triangular or 9-node quadrilateral elements (quadratic elements as shown in Figure 6). The nine node element, a continuous quadrilateral, was used in this study. The nodes are read in, and the boundary conditions are then applied to the nodes. Each element therefore consists of a list of 9 nodes in the order shown below.

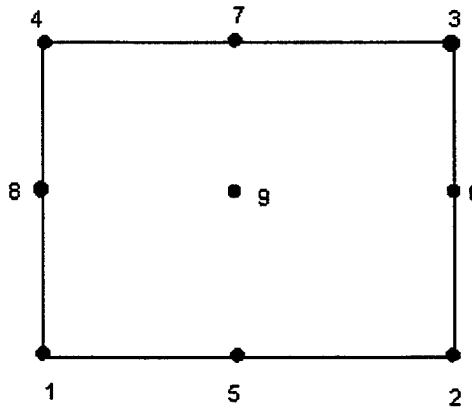


*Figure 6--Local node numbering for a nine node continuous quadrilateral element.*

### ***Cube Trial Runs***

Because an analytical solution could be performed for a cube where one boundary condition was prescribed temperature and the other boundary condition was prescribed temperature gradient (flux if the conductivity is known), a cube was used to begin the meshing process and initial code trials. The cube was specified as follows:

- i.) Domain  $0 < x, y, z < 2$
- ii.) Boundary conditions
  - at  $x = 0, T = 100 \text{ } ^\circ\text{C}$
  - at  $x = 2, \frac{dT}{dx} = 5 \text{ } ^\circ\text{C/mm}$

A continuous quadrilateral element identified as IELTYPE=40 contains 9 local nodes numbered counter-clockwise from the lower left corner as shown in Figure 6.

For the cube we started with a simple mesh which had 6 elements (one per cube face). This was generated by hand. Mesh element area was then decreased by factors of 4. Eventually, cube meshes were generated with 4, 16, 64 and 256 elements per face. Results were calculated for up to 64 elements per face.

The overall process was defined during implementation of the cube. Briefly, the input file was formed by employing COSMOS/M mesh generating software. The global node, x,y, and z coordinates, and the local node number were derived from this software package. Next, a conversion of this data into the input format for nplot3d.f was performed using a conversion program. This conversion program forms the file into the format described in Ingber[6]. Initial trials of the input file resulted in erroneous output (vs. the known analytical solution). It was determined that certain elements were indexed in a clockwise fashion and/or the combining of elements to form the cube resulted in inside-out placement of an element. Therefore, the conversion program was adapted to check for this error. If the surface normal for all elements pointed into the cube such that the numbering of local nodes is in the counter-clockwise manner specified, the elements combined together in the proper manner. Rerunning the code after the conversion program implemented checking and correction for this error, the correct results were obtained.

### ***Mesh Generation***

The tool used for mesh generation, GEOSTAR, is part of a commercial FEM package COSMOS/M [2]. Like all such packages, it is comprised of a three dimensional solid modeler plus facilities for associating a variety of elements with the solid geometric models. Fortunately, the library of elements included a nine-node shell element that provided most of the characteristics needed for the BEM code. Activities involving the GEOSTAR code were run on a Macintosh PowerPC 8100/100. Files generated were then handed off via electronic mail to a Compaq Pressario 1080, where a file conversion package written in C++ was used to convert them to a format appropriate for the BEM code. The code was run on a variety of platforms including the IBM RS6000, the same Compaq used to convert the GEOSTAR files, and on a Pentium based desktop computer where the original FEM work was completed to give a better relative computational time comparison. FEM runs of less complex meshes were also run on the Macintosh PowerPC 8100/100.

The general procedure in developing the mesh involved:

- i.) Generating a geometric model based upon key points, curves between the key points, and finally surfaces defined by the curves.
- ii.) Once these surfaces were defined, elements and their underlying nodes could be generated. Normally, a material group and its associated physical properties are defined before meshing a group of elements. This was not strictly necessary for this problem, since the full FEM package was not going to be used, however, it was found convenient to do so in order to mark

elements with an identifier that would enable their easy selection based upon the differing types of boundary conditions to be added later.

iii.) Because some of the surfaces were generated by parallel replication of already existing surfaces, their surface normal was not always consistent relative to inside vs outside the pin fin. An example would be the inside vs the outside surface of the shell, or opposite cut edges of the shell. Hence the elements which were subsequently generated on generated areas were not necessarily oriented correctly to give the counterclockwise nodal numbering scheme expected by the BEM code. Two approaches were used to rectify this situation. The first was to use the file conversion code, and the second was to determine the orientation of selected elements on a surface (all the nodal numbering sequences on a given surface were consistently numbered) by looking up the nodes associated with a given element and noting whether they were correctly ordered. Needless to say this was somewhat laborious. An alternative was found as part of activities associated with figuring out how to plot the data output by the BEM code. As part of that activity, it was desirable to generate an output file for a pin fin model so we could replicate its structure. A simple thermal model was built, and it was found that the 9-node shell element was not compatible with a thermal heat flow analysis (though it would allow thermal loading to determine expansion/contraction). Wishing to generate an output file and not having any other 9-pt elements, the simplest alternative loading was tried, that of applying a hydrostatic pressure. It was then noticed that the vector arrows used to indicate the pressure loading were pointing outward on those elements which needed to be flipped, and pointing inward on those which were correct. Once these elements were identified, COSMOS/M provides a simple command which allows inverting their 'direction'. Thereafter, this approach was applied before moving on to the next operation.

iv.) After the individual groups were identified by nodal and elemental numbers, nodal merging was accomplished. This basically merged collocated nodes on adjacent surfaces which did not have differing boundary conditions. On those common boundaries where the boundary conditions did change, this was not done. The operation of merging could be done exclusively between nodes of a single material group, by issuing a command letting them merge only among nodes of their own group. Once the merging operation was completed, a renumbering (compression) operation was performed to renumber the nodes consecutively and fill in the spaces left by those nodes, which had been subtracted by the nodal merge operation. A listing of a typical COSMOS/M session file is included in Appendix B.

### ***Mesh Conversion***

As noted, COSMOS/M has automatic mesh-generation tools that proved simple to use for mesh generation over the cube or pin fin surface, and provided quadratic 9-node shell elements, as required by the BEM code (see Figure 6). However, the FEM model grouped the elements by boundary condition, rather than nodes.

A conversion routine (see Appendix C) was formulated in C++ to convert the FEM model to the BEM input file format. This C++ code, referred to herein as the mesh converter, reads all of the nodes and elements from the COSMOS/M nodelement list file into memory, cross references the nodes and elements, and prints them in the proper BEM format. The code also prompts the user for the boundary conditions, and performs limited data validation. The data

validation includes searching for backward elements and checking for conflicting boundary conditions. Two elements can share the same node only if the elements have the same boundary conditions. If differing boundary conditions are desired, the node must be duplicated rather than shared. A warning is given, and the first boundary condition is applied. The mesh converter does not fix warnings of this type; a return to COSMOS/M is necessary. Duplicate nodes should always be used when the boundary conditions are not continuous (i.e., at an edge).

As noted above, early in this program a significant problem encountered was the difficulty in determining if all of the elements were numbered in the correct order (counter-clockwise as shown in Figure 6 rather than clockwise), i.e. that all of the surface normals were outward. Eventually, the method described in the previous section (using GEOSTAR and pressure loading) was used to solve this problem. However, an alternative method was written into the mesh conversion program (and which subsequently served as a check on the GEOSTAR procedure).

The first step in this validation is to find the center of "mass" of the nodes, by simply averaging their locations. Then, two vectors are formed on the surface of the element, one from the center node (9) of the element to the first node (1), and one from the center to the second node (2). The cross product of these vectors creates a normal vector. Then the dot product of this normal and a vector from the center of mass to the center of the element is determined. If the dot product is positive, the normal is pointing away from the center of mass. In the case of the pin fin assembly, some correctly-pointing elements (top face of the flat plate) gave negative dot products because the center of mass was too high in the pin. Therefore, the user can input an alternative center for checking. A "hidden" and potentially dangerous feature is the capability to reverse these backward elements. This feature is accessed by pressing a lower-case f (for "fix") when prompted whether a new center location is desired. Then, any elements found to be backward when compared to the new center will be repaired. It is safer to use the conversion program's feedback and actually repair the model in COSMOS/M instead. There the graphical results can be examined for errors before proceeding to the next step.

The conversion routine is also used to apply the boundary conditions to the nodes. The nodes are associated with elements, and the elements are grouped by COSMOS/M for different boundary conditions. The possible choices are specified temperature (nbdy=1), specified temperature gradient (nbdy=2), and mixed, or convection, conditions (nbdy=3). If a flux is specified, it must be divided by the material conductivity (k) to get a temperature gradient. For convection boundary conditions, the BEM method uses the following equation:

$$\phi(x) + \beta(x)\phi'(x) = \gamma(x)$$

where:

$\phi$  is the process variable (Temperature in our case)

$\phi'$  is  $d\phi/dx$

In a heat transfer problem,  $\beta$  is  $k/h$  where  $h$  is the convective coefficient and  $\gamma$  is the free-stream temperature of the gas. The gradient ( $\phi'$ ) can be expressed as a flux by multiplying by the thermal conductivity of the material modeled. The converter routine prompts for each parameter for each element group, using free-form (white space-delimited) input.

As can be seen in the code in Appendix C, the conversion routine is implemented as three classes. The first two are an element class and a node class. Arrays of these items are stored in the third “model” class. Operations included allow cross-referencing, reading, and outputting the nodes and elements. The model contains allocable arrays of nodes and elements, so the permissible size of the nodal arrays is limited only by available memory.

### **Data Visualization**

An initial attempt was made to display the results of the BEM calculation using MatLab[8]; while MatLab is a very powerful package for scientific and engineering calculations and their display, it is also a package with a steep learning curve. The basic problem with it seemed to be that while results could be plotted in 3D with pre-loaded function calls, they needed to be on a uniform grid, and the nodal points (and results) were not on such a grid. Further, piecing together (or displaying separately) the several parts of the pin fin was difficult, although easy for the cube. Therefore, other methods were sought.

Several other packages (including Mathematica[9]) were considered before it was realized that the best approach was to use the plotting routines inherent to the mesh generation package. The COSMOS/M user-provided data plotting facility offered two options. One could either enter node-defined inputs or element-defined inputs. The nodal approach actually is still plotted on elements (more about this later), but when a nodal approach is chosen, the values plotted across the elements are interpolated between the nodal values. In contrast, when the elemental approach is used, the elements show only a single value. Thus the result has a mosaic like pattern. The nodal viewpoint is better for some approaches and was desirable because nodal temperatures (the output of the BEM code) were of interest. The elemental approach also has its benefits, primarily in displaying boundary conditions that are element related. In the data file structure a flag was to be set which would tell the plotting routine which was desired. The documentation had this flag reversed.

As noted above, the nodal results are plotted in an elemental manner using internodal interpolation. One additional observation is that the elements are plotted as planes, even if the elements are not planar. This only occurs when higher order elements (such as the 9-node element) are used. It is probable that the plotting routine was developed for square or triangular 4 and 3 node elements. The net effect is that while the non-corner nodes for the cylindrical portions of the pin fin are actually on a cylindrical surface, they are represented as being polygonal. This only becomes evident on relatively coarse meshes, such as the 1/2 and 1/4 mesh models.

### **Pin Fin Analysis**

A nominal mesh size was selected for the first BEM pin fin model, with about 970 surface nodes. Additional meshes of greater and lesser nodal densities were used, with a total span of 16:1 in mesh density. The nominal model is referred to as the 1X model. The additional models were labeled 1/4X and 1/2X for the sparser models and 2X and 4X for the denser meshes. Work with the 4X mesh was limited because of the long computational times. Figure 9 shows the various meshes used.

In using the COSMOS/M mesh generation tool, five different element groups were identified. The different element groups facilitate the application of boundary conditions in the BEM model. The element groups used are:

- i.) The inside surface of the heat exchanger shell (i.e. the bottom surface of the pin fin). This was modeled as a surface without curvature. Given that the diameter of the heat exchanger is 3" for the prototype and 18" for the full scale, and the area of interest is  $\frac{1}{4}$ " wide, the amount of actual curvature was inconsequential. This surface coincides with the wall-wick interface in the heat pipe. It is maintained isothermal by evaporating sodium supplied by the capillary wick. The heat flux distribution along this surface was however of great interest in determining the performance of the heat pipe wick.
- ii.) The 'cut' surfaces of the square HX plate. Since these are symmetry boundaries with the adjoining pins that comprise a square array, they are treated as adiabatic barriers.
- iii.) The outside of the heat exchanger shell (i.e., flat surface). This is exposed to the hot gas, and is treated as a convective boundary condition with a constant convective coefficient and constant bulk fluid temperature.
- iv.) The cylinder or the cylinder plus conical fillet representing the weld. This is also exposed to the hot gas, and is likewise treated as a convective boundary condition. However, the coefficient was not necessarily going to be the same as the outside of the shell (group iii above), hence a different element group was used. In the session file generating the mesh, the diameter of the circle linking the pin to the shell was easily changed, leading to either a straight cylinder or the filleted cylinder used to approximate the weld.
- v.) The top of the pin. This is again an adiabatic surface, though it is adiabatic by reason of being insulated, not because of symmetry conditions.

The boundary conditions in Table 1 were therefore specified on the pin fin groups.

### ***Finite Element Method applied to Pin Fin***

In addition to the original COSMOS/M FEM calculations for the non-filletted pin fin case, a few varying mesh density steady state thermal FEM calculations were also made. The intent was to see how much simpler the FEM mesh could be made and still retain the essential features of the solution. These calculations were run on a Macintosh PowerPC 8100/100, and also employed COSMOS/M (V1.70A). The meshes used were similar but not identical to those used for the BEM calculations. We attempted to match the surface density of nodes and elements to the BEM approach for comparison. The same (constant) values for thermal properties and boundary conditions were used (see Table 1) as for the BEM approach.

The FEM method requires basically the same steps as the BEM; 1) define the geometry (solid, rather than surface only, however), 2) define the element and its physical properties, 3) mesh the geometry, 4) set the boundary conditions, 5) set the solution parameters (no. of iterations, tolerances, etc.; COSMOS/M's default values were used), 6) run the solution, and 7) evaluate the output.

Table 1--Boundary Conditions for Pin Fin

Bottom Surface Constant T = 750°C on Sodium side	The two-phase nature of a heat pipe working fluid makes constant temperature a good approximation. The wick thickness is ignored. Some vapor generation within the wick increases the effective conductivity of the wick.
Flat surface Constant source temperature = 1627 °C Constant Convective Coeff. = 1e-4 W/mm²°C	The thermal conductivity of the Haynes-230 alloy is high enough that slight variations in the convective term are “smeared” by thermal conduction. The BEM model can support a position-dependent convective term, but it was not deemed necessary here.
Cylinder/Filleted Cylinder Constant source temperature = 1627 °C Constant Convective Coeff. = 2e-4 W/mm²°C	Similar to above. The energy removed by one row of pins is small relative to the total energy within the gas stream, so a constant temperature source is reasonable.
Cut Surfaces Adiabatic edge conditions $q=0$ (or $dT/dn = 0$ where n is the surface normal)	Side-to-side symmetry exists. Longitudinally, while not symmetric, the differences from row to row of pins are slight, so symmetry can be assumed. The gas temperature is slightly reduced for each row, so the pin temperature is slightly reduced as well. The thin plate is not a good conductive path.
Adiabatic top surface $q=0$ (or $dT/dn = 0$ where n is the surface normal)	Insulated in real device. Leakage through insulation is small, and countered by gas leakage along pin tip.

## Results

### Cube Results

As a demonstration that the BEM code, the mesh generation method, and the mesh conversion code worked, the results of the cube problem with 64 elements per side are plotted in Figure 7 a and b. The boundary conditions are: bottom surface ( $z=0$ ) at a prescribed temperature of 100 °C, top surface ( $z=2$ ) with a prescribed normal gradient of 5 °C/mm, and all transverse surfaces with zero normal flux or gradient. The BEM program calculates a linear temperature gradient between the bottom and top surfaces, with the top surface at 110°C. This result is in agreement with the analytical solution to LaPlace's equation:

$$u''(z) = 0$$

which yields 100°C at  $z=0$ , 105°C at  $z=1$  mm, and 110°C at  $z=2$  mm (see Figure 7b) with a constant gradient of 5°C/mm. The calculated gradient out the bottom surface is shown in Figure

7a to be  $-5 \text{ }^{\circ}\text{C/mm}$  (the negative sign results because the surface normal is opposite to the z direction). Please note that Figures 7a and 7b are flipped with respect to the z axis in order to show the calculated value (rather than the specified boundary condition value) as the 'front' surface of the cube. The results of the cube problem did not vary with mesh size.

Some sources of error in the analysis became apparent from output data of the cube. The boundary integral equation developed satisfies the Laplace equation identically within the interior of the domain, and boundary conditions are equally well satisfied at the collocation nodes of the boundary. Between the collocation nodes, shape functions are used to approximate the function in the integral, and these approximations can introduce error. This approximation error can then in turn cause quadrature error, when the equations are integrated. Also, there are additional sources of error in the geometrical errors inherent in locating nodes and elements in space, and in the floating point mathematical operations needed to carry out such a calculation.

As an example, large quadrature errors resulted from a coarse mesh of one element per side. The quadrature error warning results from high errors calculated during the numerical quadrature routine for post processing at collocation points. The solution at a point towards the center of the cube was easily approximated using the quadrature routine, but as the point moved closer towards the surface the approximated solution decreased in accuracy and warnings due to large severity numbers were obtained in the program output. In Figure 8, note that the severity number increased with increase in Z towards the upper boundary at 2. The large severity number is a program check to provide the user with an understanding of the poor ability to approximate a solution at a given collocation point because the distances between the collocation point and the nodes is small. Thus, subdivision of the distance in the quadrature routine is attempted in effort to approximate the integral. For smaller subdivisions the severity number is increased. A finer mesh size reduced and/or eliminated this problem.

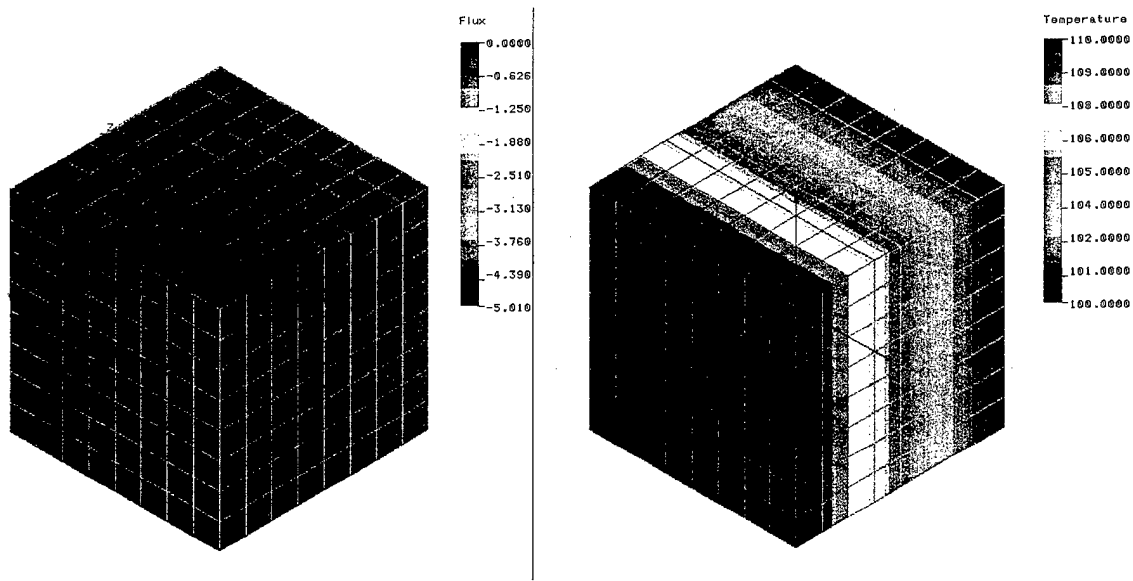


Figure 7a and b—Flux out bottom surface of cube (expressed as temperature gradient,  $^{\circ}\text{C/mm}$ ) and temperature distribution across cube ( $^{\circ}\text{C}$ ) for cube meshed with 64 elements per side.

### **BEM for cube**

*Authors: C. A. Drewien, C. Andraka, G. Knovorsky  
Date: April 19, 1997*

**MATRIX CONDITION NUMBER = .1058E+03**

**SOLUTION VALUES AT SELECTED POINTS**

**X= 1.0000 Y= 1.0000 Z= 1.0000 PHI= .105000E+03 X= .300000E+01**

**WARNING, SEVERITY NUMBER = 16**

**X= 1.0000 Y= 1.0000 Z= 1.5000 PHI= .107498E+03 X= .350000E+01**

**WARNING, SEVERITY NUMBER = 32**

**X= 1.0000 Y= 1.0000 Z= 1.7500 PHI= .108332E+03 X= .375000E+01**

**WARNING, SEVERITY NUMBER =\*\***

**X= 1.0000 Y= 1.0000 Z= 1.9500 PHI= .811817E+02 X= .395000E+01**

*Figure 8--Output of results from collocation points in the center of a cube and moving towards the top surface of the cube, which was meshed with one element per side.*

### **Pin Fin BEM Results**

The pin fin with and without a fillet were geometrically modeled and meshed using COSMOS/M software. The meshes used (with the fillet) are shown in Figure 9. The finest mesh size is referred to as 2X, followed by consistently coarser mesh sizes referred to herein as 1X, 1/2X, and 1/4X. The boundary element method was applied to the input data for the 1/4X, 1/2X, 1X, and 2X pin fins with and without the fillet.

From the results of the BEM calculations, the maximum temperature and gradient for each run were monitored. For the pin fin without a fillet, the maximum temperature, obtained on the top of the pin towards its outer edges (see Figure 10a which illustrates the 1X pin fin), was about 1038.5 °C for each mesh size. The results varied by 0.3 °C at most between the various mesh sizes, except for the 1/4X mesh (coarsest or lowest density mesh), which differed by 0.8 °C. Values of about 41.7 °C/mm were obtained for the maximum gradient out of the plate surface. Because the material of interest is a nickel-based alloy whose thermal conductivity is 0.0134 W/mm °C, the true thermal flux is obtained by multiplying these two values, i.e. 55.9 W/cm<sup>2</sup> (note change in units). A difference in flux of about 25% was observed between the maximum flux value from the finest mesh and that of the coarsest mesh, though all but the coarsest mesh results were in good agreement. Maximum temperatures and fluxes are summarized in Table 2.

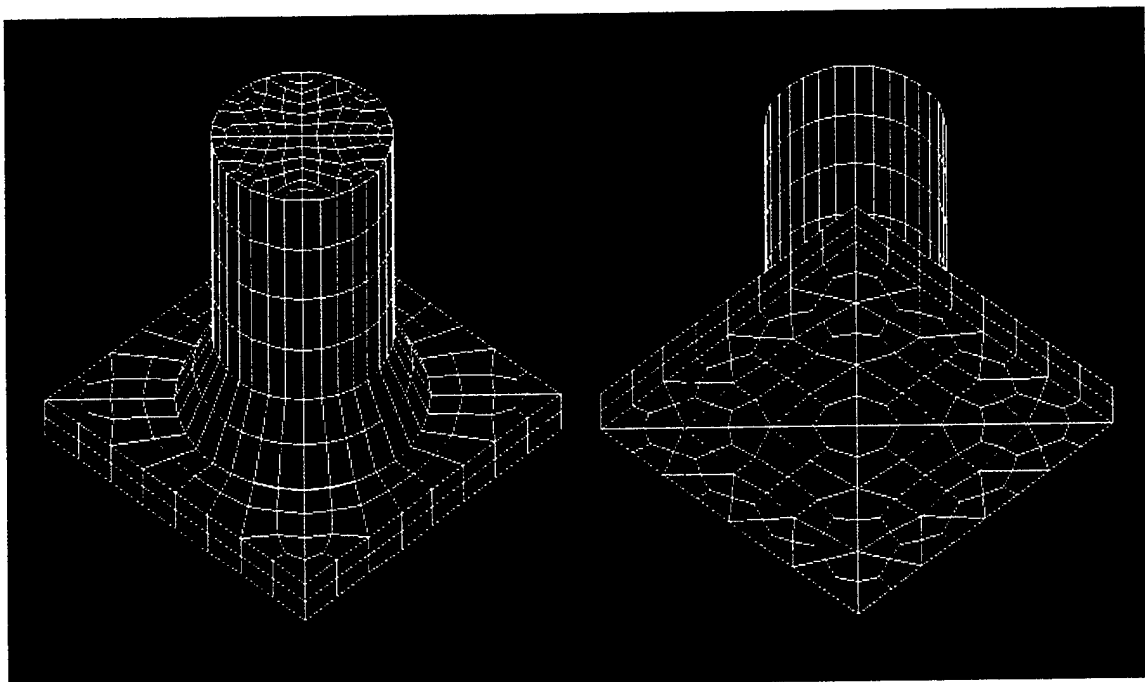


*Figure 9a. --BEM meshes of the 2X filleted pin fin model.*

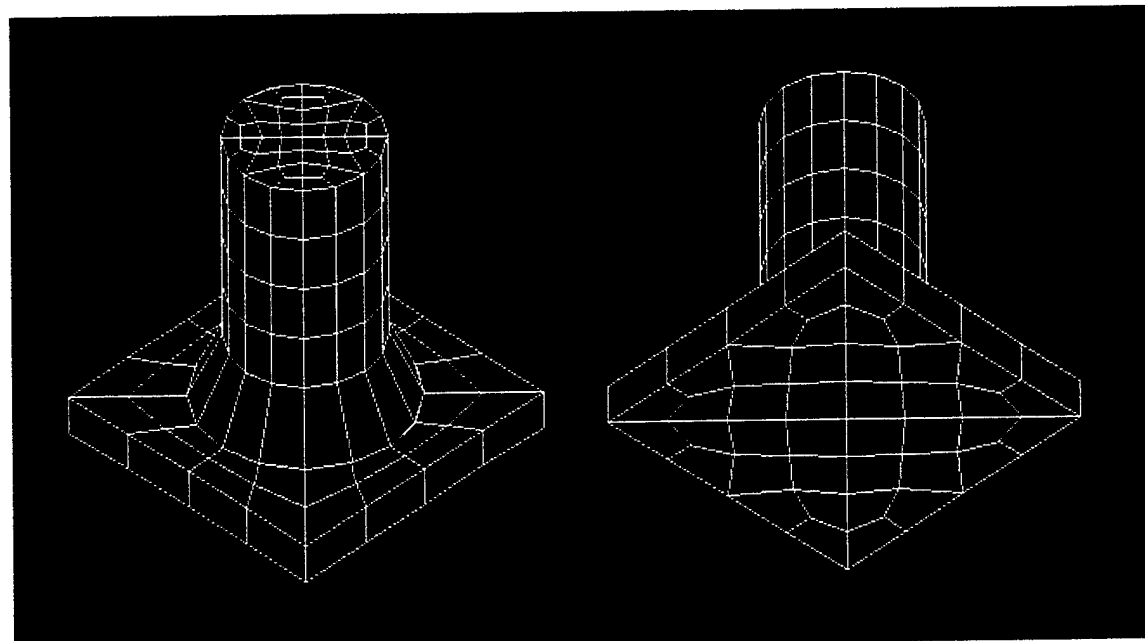


*Figure 9b.--BEM meshes of the 1X filleted pin fin model.*

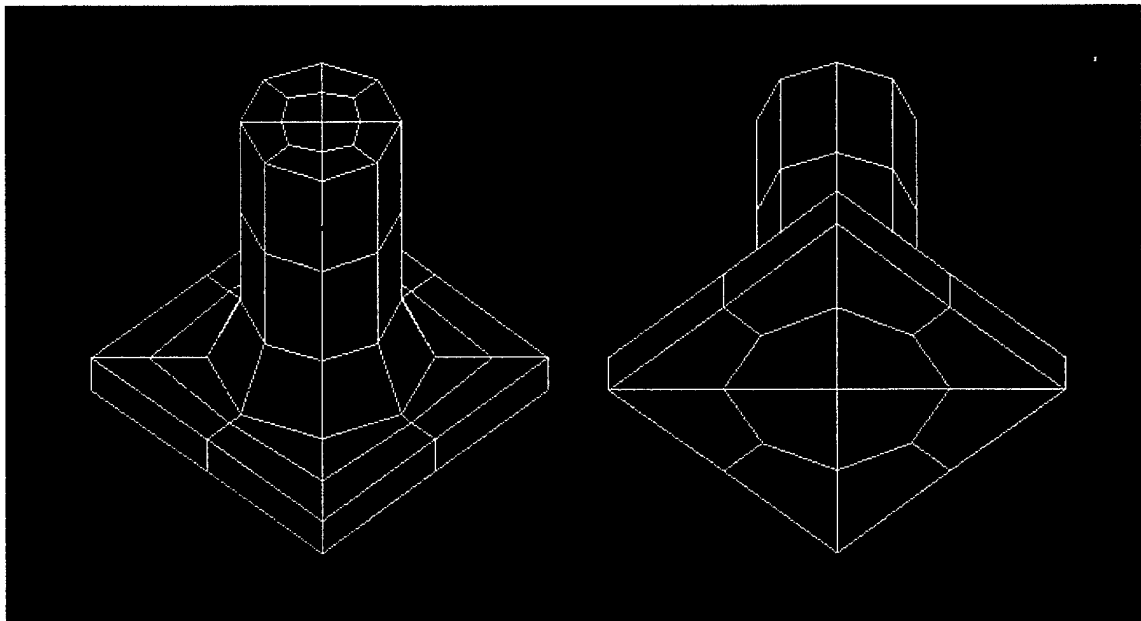


Figure 9c.--BEM meshes of the 1/2X filleted pin fin model

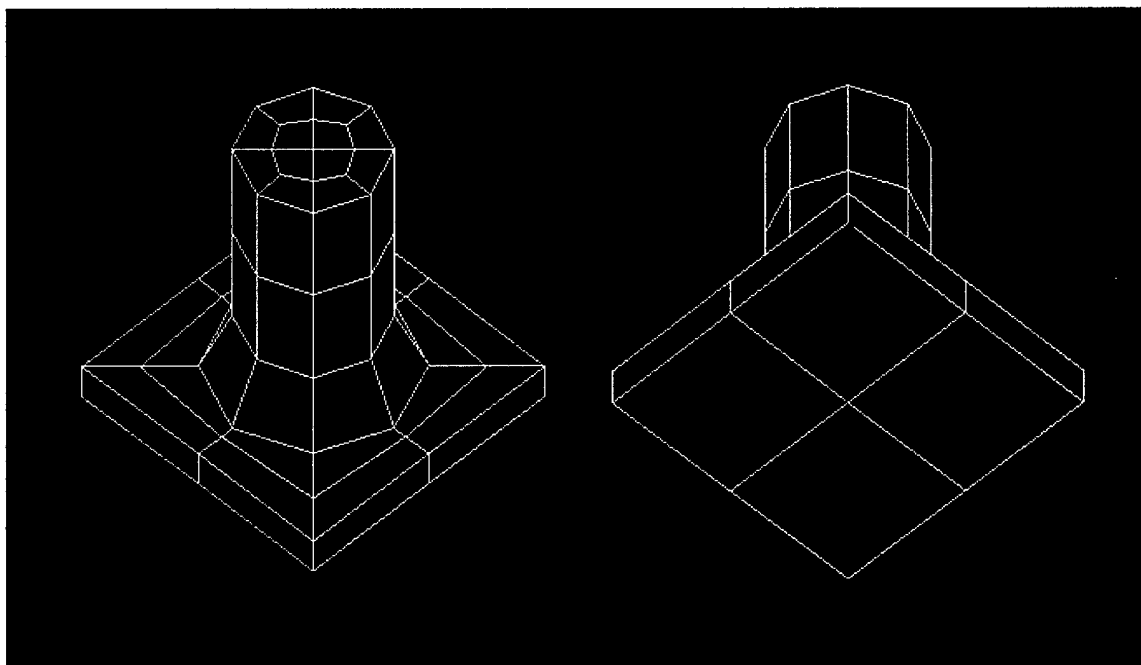


Figure 9d.--BEM meshes of the 1/4X filleted pin fin model

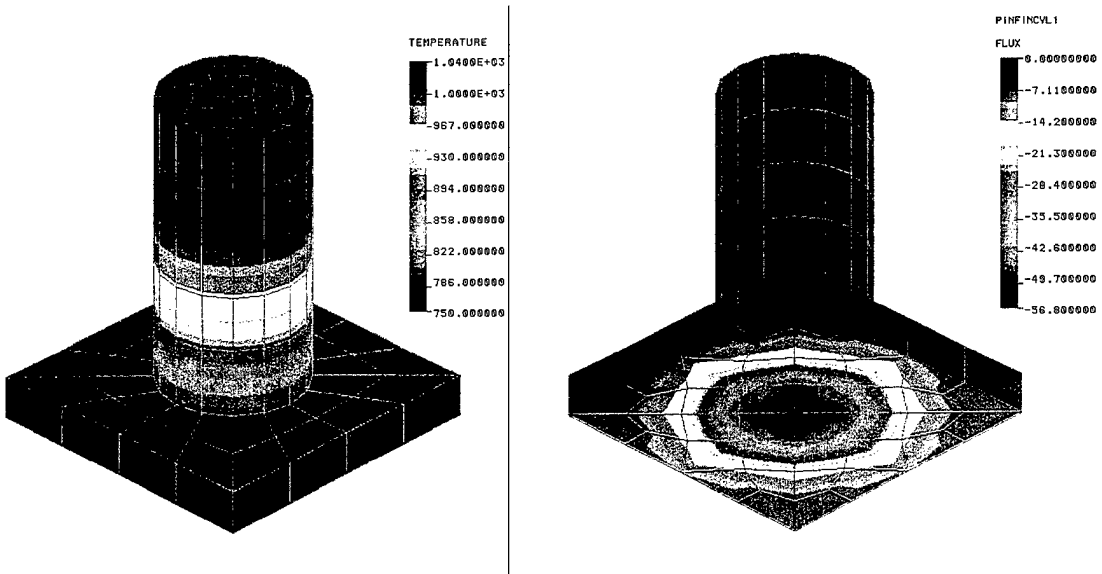


Figure 10 a and b—Temperature and gradient distribution for the straight pin fin (IX).

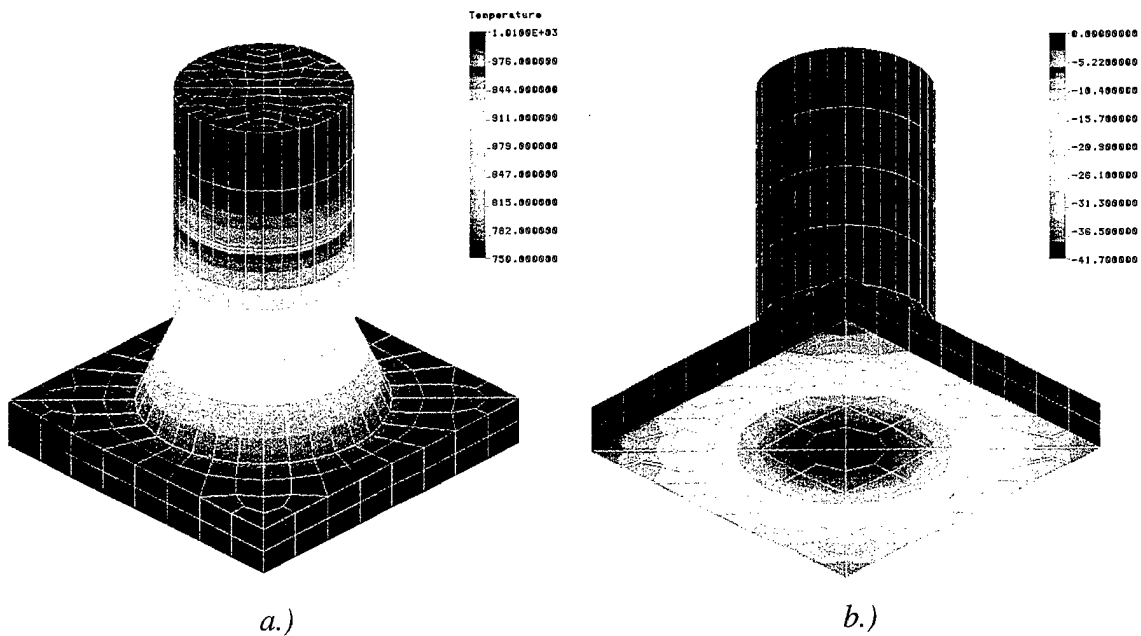


Figure 11--a.) Temperature distribution for the 2X filleted pin fin (°C). b.) Gradient distribution for the 2X filleted pin fin (°C/mm).

The pin fin with a fillet yielded lower values of peak temperature and maximum flux than the straight cylindrical pin model. For the finest mesh size, the peak temperature and gradient were 1008.1 °C and 41.7 °C/mm (or 55.9 W/cm<sup>2</sup>), respectively (see Figures 11 a and b). At the coarsest mesh size, the peak temperature and gradient were 1008 °C and 42.52 °C/mm. A 2% difference in gradient was found although little variation in temperature was detected, see Table 2.

In Figure 11 b, note the non-circular shape of the gradient distribution on the bottom surface mainly at the periphery. While a non-circular pattern over the entire plate surface is more apparent in the straight pin image of Figure 10, the latter was based on a coarser mesh. Interpolation of values between nodes is being performed by the visualization package and leads to the apparently non-circular pattern at the central region. With more nodes, the linearity would change over towards a more circular appearance. Thus, the output from visualization should always be interpreted with due respect given to the characteristic geometry of the mesh used.

Figure 12 shows the flux profile along the diagonal of the bottom surface. As can be seen, the filleted pin has very similar values for the peak flux regardless of mesh size, while the low density mesh of the straight pin has a peak flux value much different than those at the higher mesh sizes. The low-density meshes for the filleted and straight pins have only four nodal points along this diagonal. It appears to be fortuitous that the peak flux value from the low-density mesh of the filleted pin matches that of the higher density meshes. The solution is similar because the triangular shape of the low-density curve had offsetting negative and positive errors and better simulated the well-balanced bell shape of the higher density mesh cases. Thus, the lowest density or coarsest mesh (1/4X) appears too coarse for reliable results. Even though the exact solution is unknown it appears that with mesh refinement, the numerical solution is convergent to a consistent value.

The reduction in peak temperature and flux with the filleted pin fin design is the desired outcome of the pin fin models. The application of interest requires peak temperatures and fluxes to be as low as possible. The filleted pin fin better provides this combination of properties as compared to the straight pin fin. Material degradation at high temperatures results in decreased lifetime of the unit due to pin erosion by the aggressive flue gas, and higher fluxes lead to greater evaporation rates than the capillary pumping capability of the wick (which provides the sodium replacement). Lower flux reduces the rate of evaporation of sodium off of the bottom surface. Also, sodium evaporation is providing the constant temperature boundary condition at 750 °C. The filleted pin fin model is a better representation of the actual pin fin geometry. The model results show that the fillet does indeed significantly improve pin performance over the idealized pin originally modeled.

The addition of the fillet to the model decreased the peak temperature by about 3% and the peak flux by about 25%. The power throughput of the pin increased about 12%. This is primarily the result of a larger cross-sectional heat transfer area. In addition, the lower pin temperature results in a higher thermal driving potential from the free stream, again resulting in increased throughput.

### **Pin Fin FEM Results**

A series of varying mesh density FEM calculations were made for the filleted pin fin. These were run on a Macintosh PowerPC. The surface-appearance of the meshes used were similar but not identical to those used for the BEM calculations. Figure 13 shows the meshes used. In the first two cases, 8 node solid elements were used (a node at each corner), while for the last case the same mesh was used but 20 node solid elements were used instead (nodes at corners and edge

midpoints), giving an approximately 2 fold increase in surface nodal density. The 20 node element gave a better approximation to the surface nodal spacing used by the 9-node surface element BEM case (only the face center node was missing). 330, 2211 and 8325 nodes were used in the 1/4X FEM, 1/2X FEM and 1X FEM models, respectively.

*Table 2--Peak temperature and flux with mesh density. The results are for the BEM model except as noted.*

Model	Peak T (°C)	Peak Flux (W/cm <sup>2</sup> )
<b>FEM 1X w/ fillet</b>	1009	55
<b>2X w/ fillet</b>	1008	55.9
<b>1X w/ fillet</b>	1008	55.9
<b>1/2X w/ fillet</b>	1008	54.6
<b>1/4X w/ fillet</b>	1008	57.0
<hr/>		
<b>1X straight pin</b>	1038	76.1
<b>1/2X straight pin</b>	1038	76.0
<b>1/4X straight pin</b>	1039	89.6

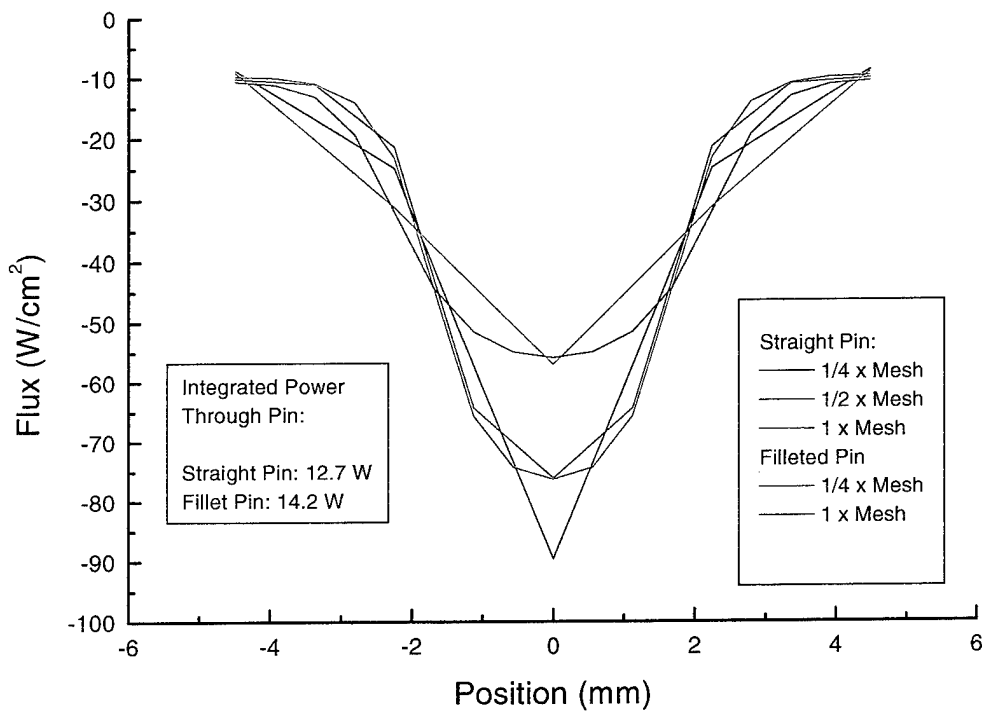
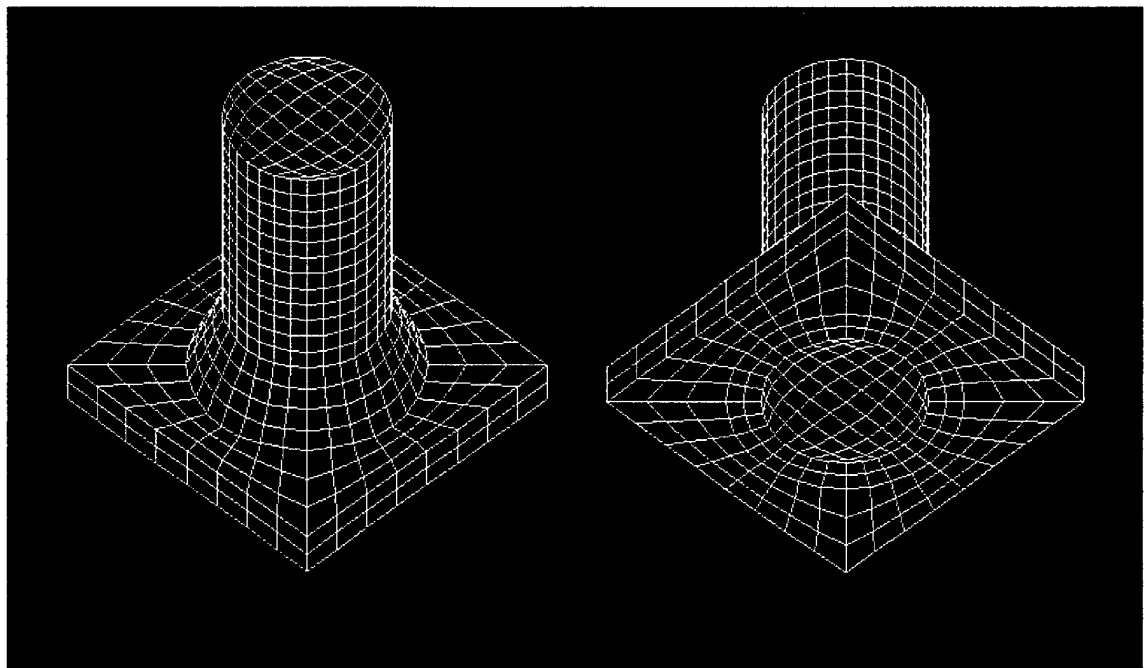


*Figure 12--Variation in BEM-calculated heat flux distribution for filleted and straight pin fins with respect to mesh density.*



a.)

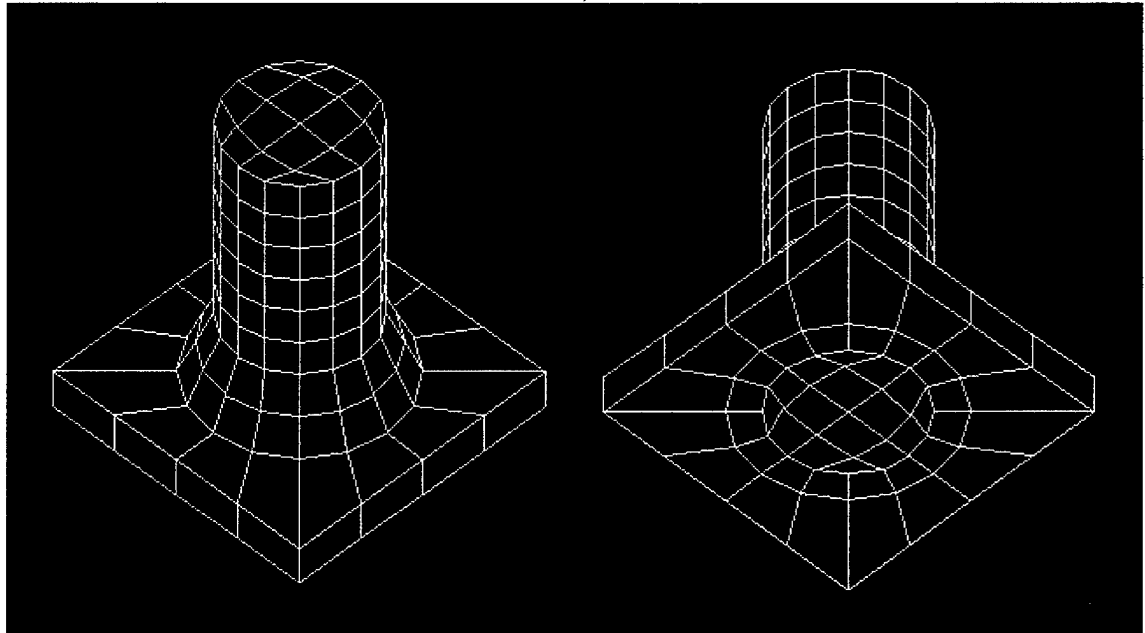
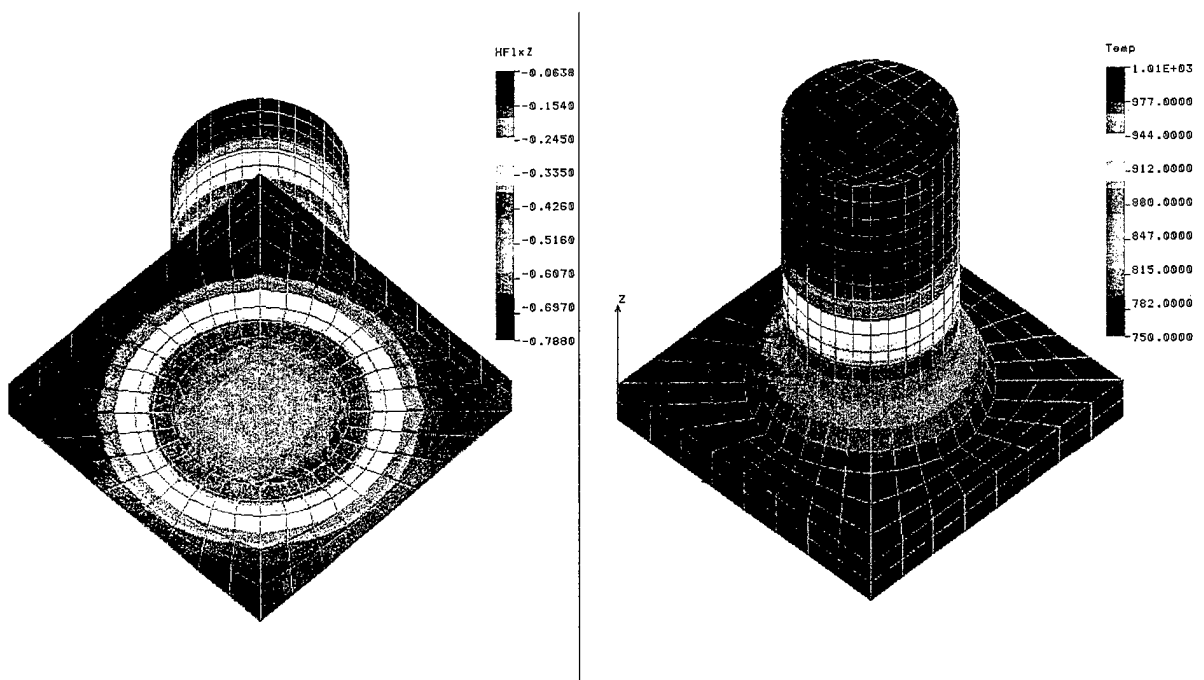
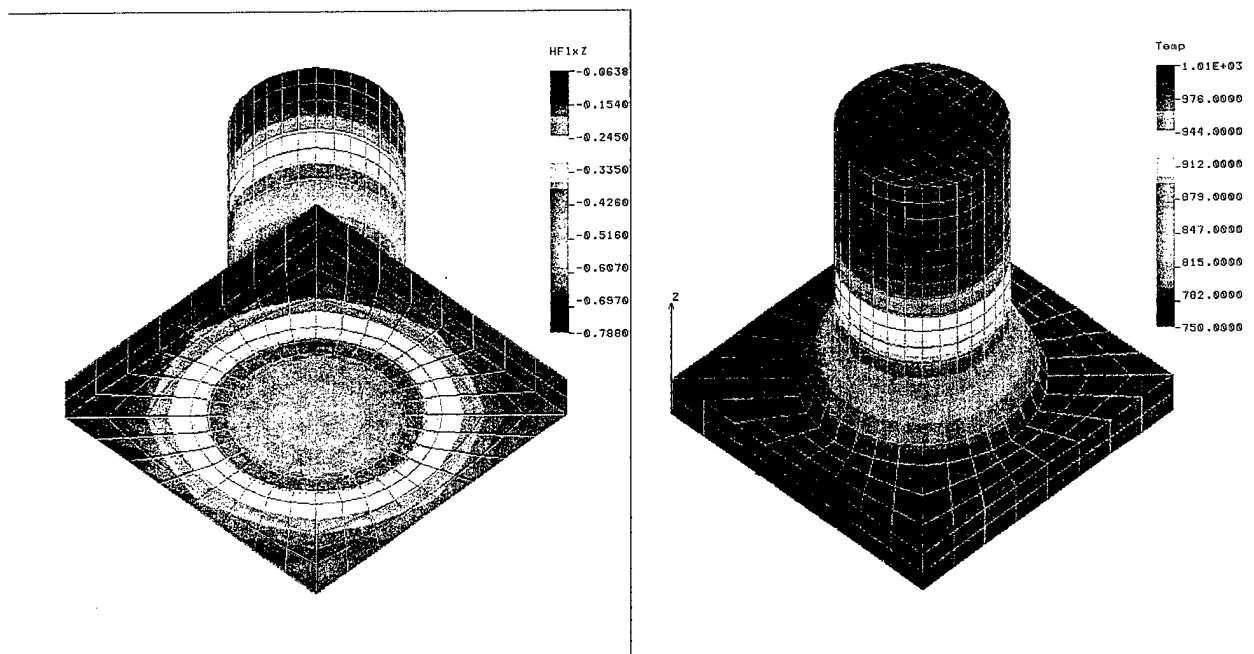


Figure 13--a.) 1X FEM and 1/2X FEM mesh (20 nodes/element & 8 nodes/element, respectively) and b.) 1/4X FEM mesh.

Heat flux (in the z-direction, parallel to the pin axis) and temperature distributions calculated by FEM are shown for the three mesh density models in Figure 14. Note that the heat flux (and not the temperature gradient) is displayed, and that it is in the z-direction, not normal to the surface. On the bottom surface this latter distinction vanishes. Compared with the BEM calculations, all three gave about the same peak temperature and location (1009.1, 1008.8 and 1009.9°C, for the 1X, 1/2X and 1/4X models, respectively).



a.)



b.)

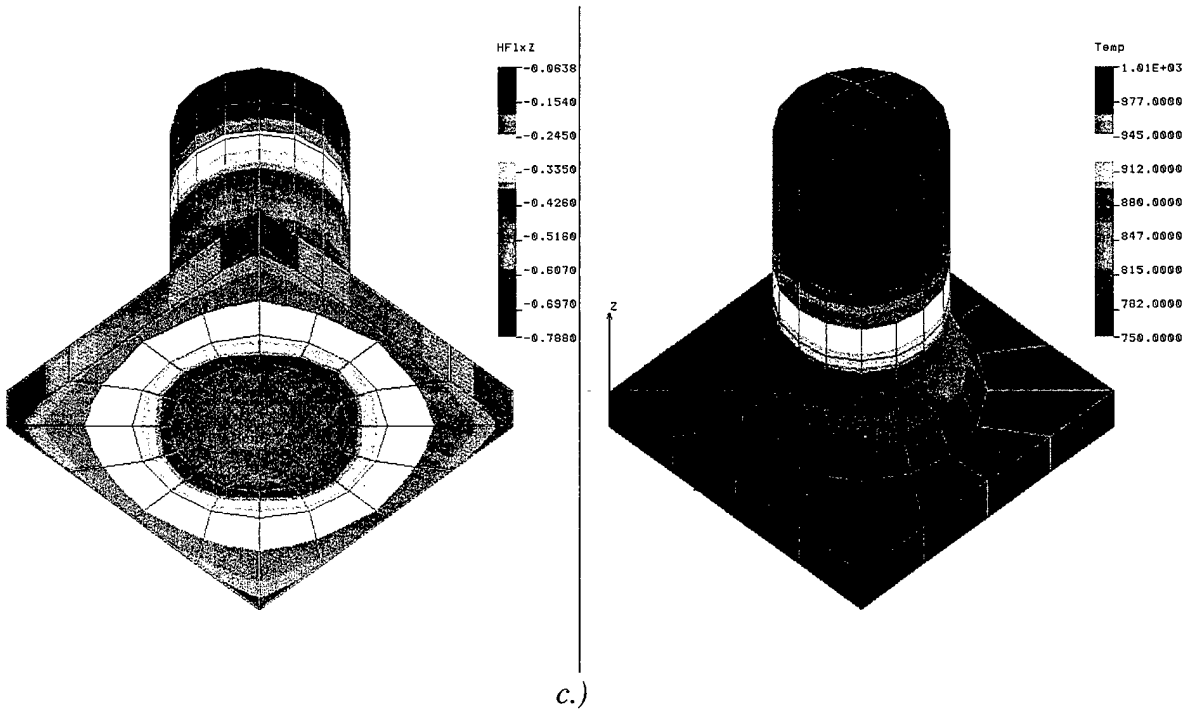


Figure 14--Heat flux in  $z$  direction ( $\text{W/mm}^2$ ) and Temperature( $^{\circ}\text{C}$ ) distributions calculated by FEM for a.) 1X, b.) 1/2X, and c.) 1/4X meshes.

Along the bottom surface diagonal, the heat flux distributions are illustrated in Figure 15:

The distance scale is normalized but correlates to the scale in Figure 12 if 0.5 is used as the zero point in Figure 12. Note that the peak value of heat flux for all three cases is quite consistent, though the minimum value (at the corners) shows a considerable variation for the least dense mesh model. Also note that the values are plotted as  $\text{W/mm}^2$ , rather than  $\text{W/cm}^2$ , as in the BEM results in Figure 12. Compared with the BEM mesh, the FEM mesh along the bottom surface is denser for the equivalent model nomenclature (set by the mesh density along the “cut” edge of the plate). This is because the surface elements of the BEM mesh on the bottom surface are completely unrelated to the elements on the other surface of the plate where the pin is located. The FEM case (which uses volume elements) cannot achieve this independence across such a thin region.

An approximate comparison of the two methods’ nodal densities on the bottom surface (by number of nodes on bottom surface) is given in Table 3.

It is apparent that the FEM density on the bottom surface is approximately equivalent to the next level BEM mesh. Judging by the results, both BEM and FEM have significant inaccuracies at the most coarse mesh condition. For the BEM the gradient is aberrant at the center, while for the FEM the problem occurs at the “corners”.

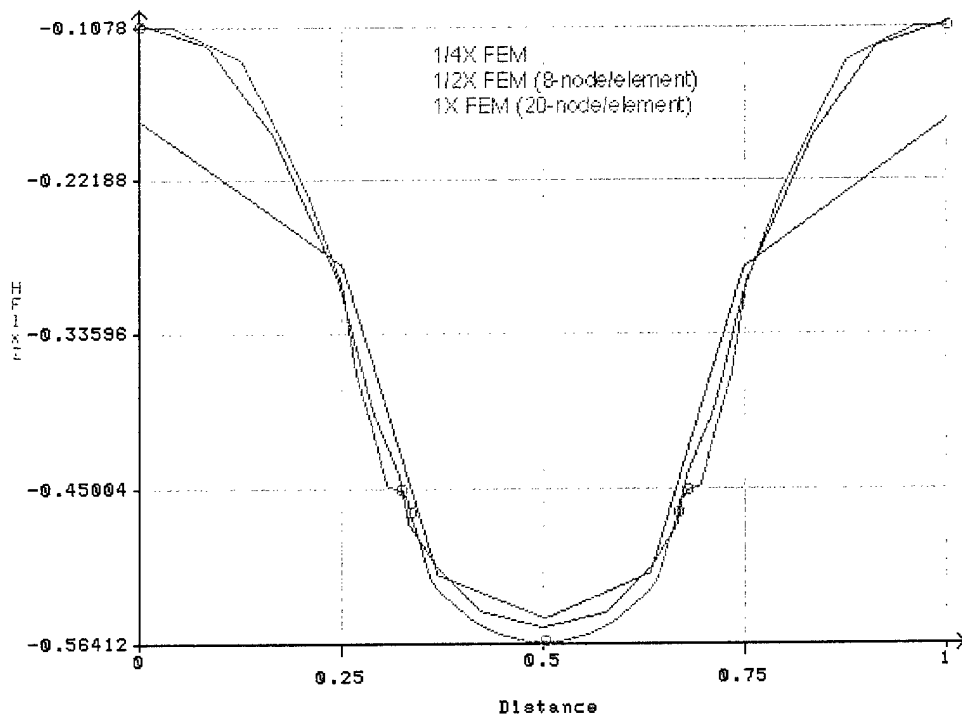


Figure 15--Heat flux in  $z$  direction ( $\text{W/mm}^2$ ) along bottom diagonal of pin fin, calculated by FEM for 1X, 1/2X, and 1/4X meshes.

Table 3--Comparison of BEM and TEM bottom surface nodal density (number of bottom surface nodes in models)

	BEM	FEM
2X	577	-
1X	177	665
1/2X	57	241
1/4X	25	57

### Timing Results

Without an optimization level for the compiler specified, BEM calculation times as long as 272 seconds were obtained for the pin fin with fillet, (1x mesh) on the RS6000 computer. To further improve the times, optimizer levels of 2 and 3 (xlf compiler) were used for compiling the executable program. It was seen that an order of magnitude decrease in timing could be obtained with a good optimizer on the BEM code. The results are summarized in Table 4.

Figure 16 a-c contains the timing results from three cube files, 3 pin fin without fillet files, and 4 pin fin with fillet files. The number of nodes vs the time (in seconds) is shown in Table 5 for all of the files. The linear curve fit of the log MATVEC time vs log nodes yielded a slope of 1.65; log DECOMP/SOLVE vs log nodes yielded a slope of 2.92; and, log total time vs log nodes yielded a slope of 2.03.

*Table 4--Comparison of BEM run times with differing levels of code optimization on the RS6000 computer.*

Optimizer level	GEOM time (seconds)	MATVEC time (seconds)	LU/SOLVE time (seconds)	Output time (seconds)	Total time (seconds)
not specified	0.18	114	160	0.06	272
O2	0.2	36	21	0.05	58
O3	0.2	33	21	0.06	54

The MATVEC subroutine uses a do loop on nodes with a call to subroutine INT4, which uses a do loop around the number of local nodes, and then performs another do loop on nodes in the main subroutine followed by another do loop on nodes. Thus, subroutine MATVEC should be order 2 (O2). The time to collect and assemble the matrices—A, B, phi, phip, etc.—is dominating the processes for the matrix sizes used in this experiment, since the overall order is about 2. With larger matrices, the LU Decomposition subroutine should eventually dominate the program and yield order three, as seen by the value of 2.92 for the slope of the log DECOMP/SOLVE vs log nodes plot. This reflects the relatively short triple do loop around the number of nodes in the LU DECOMP subroutine. Note that the SOLVE subroutine has two do loops on the number of nodes, therefore the LU Decomposition subroutine dominates the process. The memory storage process is order 2. It appears that the constant multiplier for the order 2 processes in the code dominate the smaller multiplier for time contribution from DECOMP/SOLVE, which is order 3. With larger arrays/matrix, it is expected that the overall performance should scale as order 3.

*Table 5--Output from timing tests for differing number of nodes. Results were obtained using an IBM RS6000 with an optimizer level of 2 and requesting uninterrupted use of one processor.*

Model	Nodes	GEOM time (seconds)	MATVEC time (seconds)	DECOMP/SOLVE time (seconds)	Output time (seconds)	Total time (seconds)
4 el/side Cube	150	0.03	1.43	0.1	0.01	1.57
1/4X Straight	322	0.08	6.87	0.89	0.02	7.86
1/4X Fillet	322	0.07	6.69	0.89	0.01	7.66
1/2X Straight	354	0.08	8.41	1.1	0.01	9.6
1/2X Fillet	354	0.07	8.33	1.1	0.02	9.52
16 el/side Cube	486	0.07	9.82	2.91	0.02	12.82
1X Fillet	962	0.19	36.32	21.04	0.05	57.6
1X Straight	971	0.18	37.28	21.59	0.05	59.1
64 el/side Cube	1734	0.3	89.2	125.8	0.09	215.3
2X Fillet	2562	0.53	206	394.5	0.13	601.9

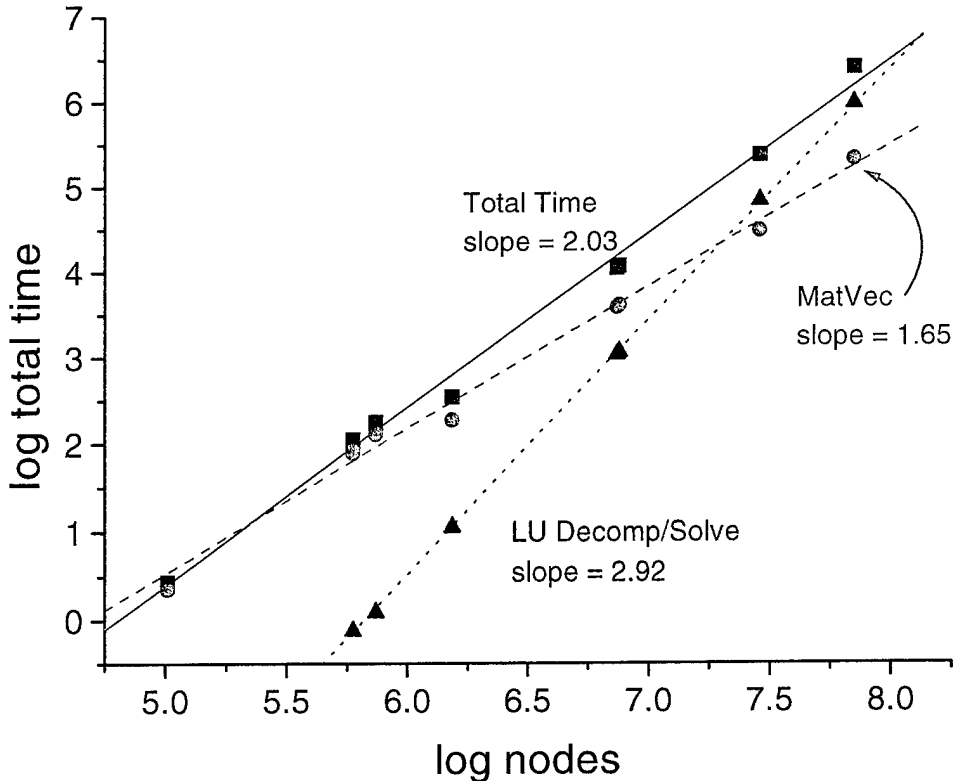


Figure 16—BEM Timing results for total time and portions of the code. Time is in seconds.

The finite element code, COSMOS/M, was used on the filleted pin fin as a comparison of results from the BEM code. The resulting times were 51 seconds total time for the FEM code using a highly optimized COSMOS/M proprietary code and an 8871-node model, 306 seconds total time for an older, non-proprietary COSMOS/M code, and 1420 seconds for the 2X pin fin (2562 nodes) BEM model on the PC. The FEM model in this case had a greater surface density of elements than the BEM model. However, the FEM model uses highly optimized code, while the FORTRAN compiler (Microsoft Powerstation FORTRAN) has limited optimization. Note that the BEM times are much slower on the PC than on the RS6000, while the computational speed of the machines are similar. These timings were performed on a Pentium 90 with 80 M of RAM. COSMOS/M is not available on the RS6000.

Further timing measurements for the less complex FEM models run on the Macintosh Power PC (with 40 M of RAM and a 100 Mhz processor) gave values of 1231 seconds total time for the 1X FEM model (8325 nodes), 138 seconds for the 1/2X model (2211 nodes) and 19 seconds for the 1/4X model (330 nodes). These times are considerably slower than the times on the PC. Most of the total time was spent assembling and decomposing the matrices; actual solution time took only about 5-7% of the total time. Plotting total time values on a log-log plot (Figure 17), the slope is found to be 1.27, which is of considerably lower order than the BEM code.

The computation time increase caused by model complexity is of order 1.27 for the FEM and 2 for the BEM. However, as the mesh density increases, the number of nodes in the FEM model increases as  $N^3$  where  $N$  is the number of nodes in a given linear direction, while the nodes on a BEM model increase as  $N^2$ . Thus, the actual order of time increase with linear node density is 3.8

for FEM and 4.1 for the BEM method. Given all the variables involved, these orders are very similar. A more exhaustive study using good optimization on the same machine would be appropriate. In addition, the accuracy of the solution would be a better comparison than surface nodal density.

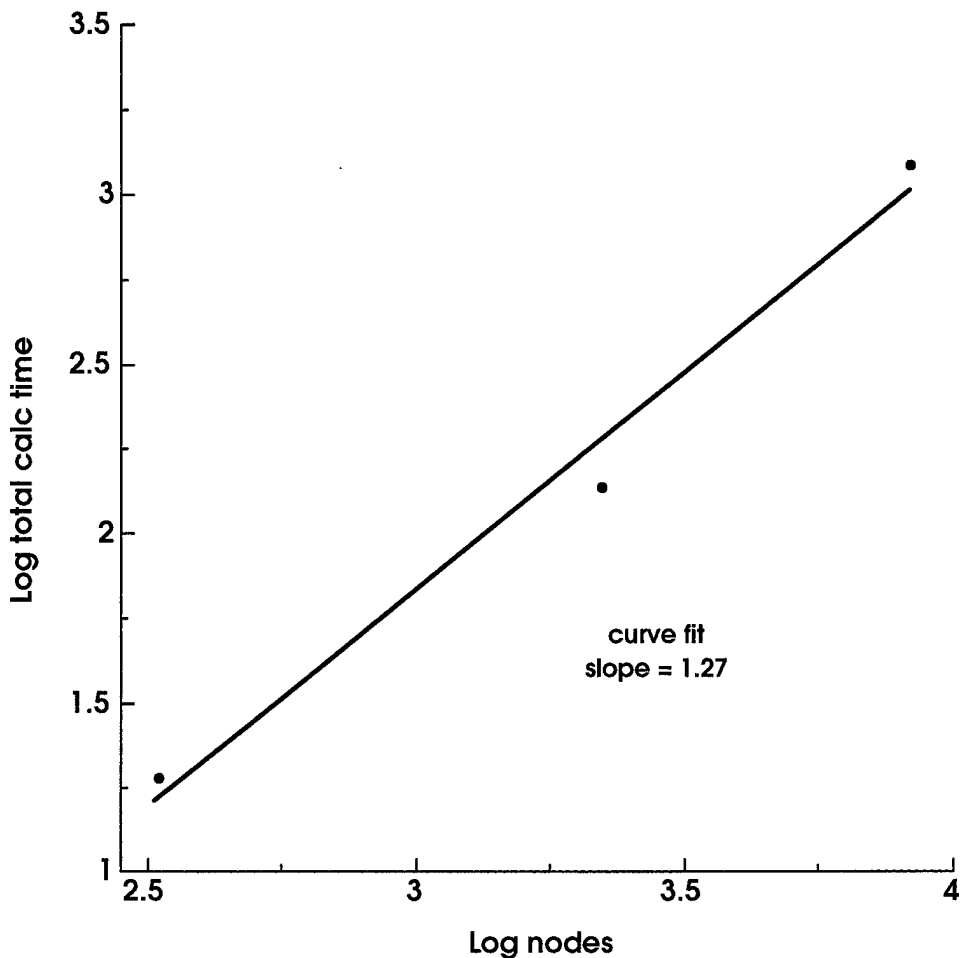


Figure 17--Total FEM calculation time vs number of nodes in model.

## Summary/Conclusions

It was determined that the weld fillet on the pin fin significantly enhanced the heat transfer to the sodium working fluid, improving the operating margin of the heat pipe. The peak flux was reduced by 25% under the worst-case scenario, while the peak pin temperature was slightly reduced, when compared to the previously modeled idealized pin fin. The reduced pin temperature and fixed gas temperature resulted in 12% more total power that could be transferred by the pin. These significant changes in pin performance should be incorporated into the overall heat-pipe performance models, including the Fluent CFD model and the heat pipe wick model.

In the models investigated, there is not a clear advantage in computational time for either the BEM or FEM methods, though the proprietary optimized COSMOS/M FEM code on a Pentium PC appears to be the fastest method investigated. Processor speeds and code optimization capabilities differed between the machines used. A more careful study should be performed with geometries that have analytical solutions and with good optimizing compilers.

In the range of model sizes investigated, the BEM and FEM codes have similar scalability based on linear grid spacing. However, the BEM code has a higher order ( $O(3)$  based on number of nodes) routine (LU Solve) that will dominate on very large models, and thus may be less scaleable than the FEM method.

A process for performing 3-dimensional BEM analysis was developed, tested, and applied to the problem at hand. The process is as follows:

- i.) Model the part and perform mesh generation over the surface. (Use of the COSMOS/M program was helpful for this task, however other packages that would provide the same results are available. It is necessary to assure that surface normals are oriented properly.)
- ii.) Supply information from mesh generation to the mesh converter program in order to form an input file with the necessary format for the BEM program.
- iii.) Run Marc Ingber's BEM program (NPOT3D) with the input file and obtain an output file of node number and temperature and flux for every node.
- iv.) Graph the output file. In our work this was supplied to COSMOS/M as a user defined plotfile to obtain 3-dimensional graphing of the temperature or flux over the object surface. Limitations of the graphics output must be considered in the interpretation of data (i.e. polygonal plotting of cylindrical elements, linear interpolation of data between nodes).
- v.) Additionally, information such as peak temperatures and flux can be obtained directly from simple sorting or statistical analysis of the data in the output file.
- vi.) The BEM solutions at points inside the object can be obtained by supplying the coordinates of interest into the input file. The severity number indicates accuracy of the result. If no severity number is reported, the accuracy is good.

In summary, an existing FEM mesh-generation tool was used to develop complex meshes for the BEM technique in conjunction with an automated conversion routine that incorporated boundary conditions and some error checking.

## Acknowledgments

The authors thank Marc Ingber, Scott Rawlinson, Brian Smith, and Richard Allen for their help and encouragement with this work. This work was performed at the University of New Mexico, Albuquerque Resource Center, and Sandia National Laboratories, which is operated for the U.S. Department of Energy under contract number DE-AC04-94AL85000.

## References

---

- 1 Fluent UNS, West Lebanon, NH.
- 2 COSMOS/M, Structural Research and Analysis Corporation, Los Angeles, CA.
- 3 Marc S. Ingber, npot3d.f BEM code.
- 4 Diver, R.B., et al, "Trends in Dish Stirling Solar Receiver Design," paper no. 905303, *Proceedings of the 25th IECEC*, Reno NV, August, 1990.
- 5 Marc S. Ingber, SAND93-7072, Sandia National Laboratories report, Albuquerque, NM (1993).
- 6 Marc S. Ingber memo to D. W. Larson, Sandia National Laboratories, Albuquerque, NM (August 10, 1987).
- 7 High Performance Computing, Schable et al. (1990).
- 8 Matlab, The MathWorks Inc., Natick, MA.
- 9 Mathematica, Wolfram Research Inc., Champaign, IL.

## Appendix A. NPOT3D BEM Code

```
C=====
C  NPOT3d.f
C
C  This program solves Laplace's equation in a three-dimension
C  interior or exterior domain using the Direct Boundary Element Method.
C
C  Data for the program is supplied from the data file FLOW3D.DAT.
C  Output is written to the file FLOW3D.OUT.  For the proper format for
C  the input file, see
C
C
C  Dimensioning Notes:  The program is currently dimensioned for a
C                      maximum of 4001 nodes and 1001 elements.
C                      These limits can only be increased by
C                      changing the appropriate DIMENSION statements
C                      in the program.
C
C  Written by:  M. S. Ingber
C                  University of New Mexico
C                  Department of Mechanical Engineering
C                  Albuquerque, New Mexico 87185*
C
C=====
COMMON /VARS/ PI,INTFL
COMMON /QUAD/ SQPT,TQPT,WGT,GPT,SWGT
COMMON /NQUAD/ GP(12,8),GW(12,8),NSEV(8)
COMMON /TQUAD/ SGP(112,8),TGP(112,8),NSEV2(8),GWT(112,8)
DIMENSION X(4001),Y(4001),Z(4001),IJK(9,1001),IPVT(4001)
DIMENSION WK(4001),A(4001,4001),B(4001),IELTYPE(1001)
DIMENSION SQPT(7),TQPT(7),WGT(7),GPT(4),SWGT(4),PHIP(4001)
DIMENSION PHI(4001),BET(4001),GAM(4001),NBDY(4001),ICFL(4001)
DIMENSION XACP(200),YACP(200),ZACP(200)
DIMENSION *8 root
character *8 root

real t1,t2,t3,t4,t5,t6

print *, 'Enter file root name: '
read *,root
OPEN(UNIT=5,FILE=root//'.dek',STATUS='old')
OPEN(UNIT=6,FILE=root//'.out',STATUS='unknown')
OPEN(UNIT=3,FILE=root//'.plt',STATUS='unknown')
OPEN(UNIT=2,FILE=root//'.flx',STATUS='unknown')
PI=4.*ATAN(1.)

CALL QUADR
call mytime(t1)

CALL GEOM(X,Y,Z,IJK,NODES,NE,PHI,PHIP,BET,GAM,IELTYPE,
A           NBDY,ICFL,XACP,YACP,ZACP)

call mytime(t2)
CALL MATVEC(X,Y,Z,IJK,NODES,NE,A,B,PHI,PHIP,BET,GAM,IELTYPE,
A           NBDY,ICFL,XACP,YACP,ZACP)

call mytime(t3)
CALL DECOMP(NODES,COND,IPVT,WK,A)
CALL SOLVE(NODES,B,IPVT,A)

call mytime(t4)
C  Write the solution vector to a plot file
do i=1,nodes
```

```

        if (nbdy(i).eq.1)then
C          Specified T: temperature is given
C          write(3,*)i,phi(i), b(i)
C          write(2,*)x(i),y(i),z(i),b(i)
        elseif(nbdy(i).eq.2) then
C          Specified flux: Temperature is solution vector
C          write(3,*)i,b(i), phi(i)
        else
C          Convection: solution is phi prime
C          write(3,*)i,gam(i)-bet(i)*b(i)
        end if
      end do

      WRITE(6,300) COND
300 FORMAT(' MATRIX CONDITION NUMBER = ',E14.4)

      call mytime(t5)
      CALL CALPHI(X,Y,Z,IJK,NODES,NE,B,PHI,PHIP,BET,GAM,
A          IELTYPE,NBDY)

      call mytime(t6)

      write(2,400) t2-t1
400 format('geom time  = ',E10.4)
      write(2,401) t3-t2
401 format('matvec time  = ',E10.4)
      write(2,402) t4-t3
402 format('LU and solve time  = ',E10.4)
      write(2,403) t5-t4
403 format('output time  = ',E10.4)
      write(2,404) t6-t5
404 format('collocation time  = ',E10.4)

      STOP
      END
C
C
C
      SUBROUTINE MATVEC(X,Y,Z,IJK,NODES,NE,A,B,PHI,PHIP,
A          BET,GAM,IELTYPE,NBDY,ICFL,XACP,YACP,ZACP)
      COMMON /VARS/ PI,INTFL
      COMMON /QUAD/ SQPT,TQPT,WGT,GPT,SWGT
      DIMENSION X(*),Y(*),Z(*),IJK(9,1),A(4001,4001),B(*)
      DIMENSION AH1(4001),AH2(4001),SQPT(7),TQPT(7),WGT(7)
      DIMENSION GPT(4),SWGT(4),CCPT(3),PHIP(*),IELTYPE(*)
      DIMENSION PHI(*),BET(*),GAM(*),NBDY(*),ICFL(*)
      DIMENSION ZACP(*),XACP(*),YACP(*)
      A1=0.05971587
      A2=0.10128651
      A3=0.47014206
      A4=0.79742699
      W1=0.06296959
      W2=0.06619708
      W3=0.1125
      SQPT(1)=A2
      SQPT(2)=A3
      SQPT(3)=A4
      SQPT(4)=A3
      SQPT(5)=A2
      SQPT(6)=A1
      SQPT(7)=1./3.
      TQPT(1)=A2
      TQPT(2)=A1
      TQPT(3)=A2
      TQPT(4)=A3
      TQPT(5)=A4
      TQPT(6)=A3

```

```

TQPT(7)=1./3.
WGT(1)=W1
WGT(2)=W2
WGT(3)=W1
WGT(4)=W2
WGT(5)=W1
WGT(6)=W2
WGT(7)=W3
GPT(1)=-0.86113631
GPT(2)=-0.33998104
GPT(3)=0.33998104
GPT(4)=0.86113631
SWGT(1)=0.347854845
SWGT(2)=0.65214515
SWGT(3)=0.65214515
SWGT(4)=0.347854845
ICT=0
DO 10 I=1,NODES
  IF (ICFL(I).EQ.0) THEN
    CCPT(1)=X(I)
    CCPT(2)=Y(I)
    CCPT(3)=Z(I)
  ELSE
    ICT=ICT+1
    CCPT(1)=XACP(ICT)
    CCPT(2)=YACP(ICT)
    CCPT(3)=ZACP(ICT)
  ENDIF
  CALL INT4(I,CCPT,AH1,AH2,NODES,NE,IJK,X,Y,Z,IELTYPE)
  AH1(I)=0.0
  DO 20 J=1,NODES
    IF (J.EQ.I) GO TO 20
    AH1(I)=AH1(I)-AH1(J)
20  CONTINUE
  IF (INTFL.EQ.1) AH1(I)=4.*PI+AH1(I)
  B(I)=0.
  DO 30 J=1,NODES
    GO TO (41,51,61) NBDY(J)
C
C  NBDY(J) = 1 => PHI SPECIFIED
C  NBDY(J) = 2 => PHIP SPECIFIED
C  NBDY(J) = 3 => ROBIN BOUNDARY CONDITION
C
41  CONTINUE
  A(I,J)=AH2(J)
  B(I)=B(I)+PHI(J)*AH1(J)
  GO TO 30
51  CONTINUE
  A(I,J)=-AH1(J)
  B(I)=B(I)-PHIP(J)*AH2(J)
  GO TO 30
61  CONTINUE
  A(I,J)=AH2(J)+AH1(J)*BET(J)
  B(I)=B(I)+GAM(J)*AH1(J)
30  CONTINUE
10 CONTINUE
  RETURN
END
C
C
C
  SUBROUTINE INT4(INO,CCPT,AH1,AH2,NODES,NE,IJK,X,Y,Z,IELTYPE)
  COMMON /VARS/ PI,INTFL
  COMMON /QUAD/ SQPT,TQPT,WGT,GPT,SWGT
  DIMENSION AH1(*),IJK(9,1),CCPT(*),G1(9),G1P(9),AH2(*)
  DIMENSION SQPT(7),TQPT(7),WGT(7),GPT(4),SWGT(4)
  DIMENSION COORD(3,9),COORDT(9,3),DSQ(9),X(*),Y(*),Z(*)

```

```

DIMENSION IELTYPE(*)
SMALL=1.E-6
DO 5 I=1,NODES
  AH1(I)=0.0
  AH2(I)=0.0
5 CONTINUE
DO 10 I=1,NE
  IF (IELTYPE(I).LT.40) THEN
    NS=6
    COORD(1,1)=X(IJK(1,I))
    COORD(2,1)=Y(IJK(1,I))
    COORD(3,1)=Z(IJK(1,I))
    COORD(1,2)=X(IJK(2,I))
    COORD(2,2)=Y(IJK(2,I))
    COORD(3,2)=Z(IJK(2,I))
    COORD(1,3)=X(IJK(3,I))
    COORD(2,3)=Y(IJK(3,I))
    COORD(3,3)=Z(IJK(3,I))
    COORD(1,4)=X(IJK(4,I))
    COORD(2,4)=Y(IJK(4,I))
    COORD(3,4)=Z(IJK(4,I))
    COORD(1,5)=X(IJK(5,I))
    COORD(2,5)=Y(IJK(5,I))
    COORD(3,5)=Z(IJK(5,I))
    COORD(1,6)=X(IJK(6,I))
    COORD(2,6)=Y(IJK(6,I))
    COORD(3,6)=Z(IJK(6,I))
    DO 15 IC=1,3
    DO 15 JC=1,6
      COORDT(JC,IC)=COORD(IC,JC)
15 CONTINUE
DO 25 IC=1,6
  DSQ(IC)=(COORD(1,IC)-CCPT(1))**2+(COORD(2,IC)-
A           CCPT(2))**2+(COORD(3,IC)-CCPT(3))**2
  DSQ(IC)=SQRT(DSQ(IC))
25 CONTINUE
INODE=0
IF (DSQ(1).LE.SMALL) INODE=1
IF (DSQ(2).LE.SMALL) INODE=2
IF (DSQ(3).LE.SMALL) INODE=3
IF (DSQ(4).LE.SMALL) INODE=4
IF (DSQ(5).LE.SMALL) INODE=5
IF (DSQ(6).LE.SMALL) INODE=6
IF (INODE.EQ.0) THEN
  CALL RTINT(CCPT,G1,G1P,COORD,COORDT)
ELSE
  CALL STINT(CCPT,G1,G1P,COORD,COORDT,INODE)
END IF
ELSE
  NS=9
  COORD(1,1)=X(IJK(1,I))
  COORD(2,1)=Y(IJK(1,I))
  COORD(3,1)=Z(IJK(1,I))
  COORD(1,2)=X(IJK(2,I))
  COORD(2,2)=Y(IJK(2,I))
  COORD(3,2)=Z(IJK(2,I))
  COORD(1,3)=X(IJK(3,I))
  COORD(2,3)=Y(IJK(3,I))
  COORD(3,3)=Z(IJK(3,I))
  COORD(1,4)=X(IJK(4,I))
  COORD(2,4)=Y(IJK(4,I))
  COORD(3,4)=Z(IJK(4,I))
  COORD(1,5)=X(IJK(5,I))
  COORD(2,5)=Y(IJK(5,I))
  COORD(3,5)=Z(IJK(5,I))
  COORD(1,6)=X(IJK(6,I))
  COORD(2,6)=Y(IJK(6,I))

```

```

COORD(3,6)=Z(IJK(6,I))
COORD(1,7)=X(IJK(7,I))
COORD(2,7)=Y(IJK(7,I))
COORD(3,7)=Z(IJK(7,I))
COORD(1,8)=X(IJK(8,I))
COORD(2,8)=Y(IJK(8,I))
COORD(3,8)=Z(IJK(8,I))
COORD(1,9)=X(IJK(9,I))
COORD(2,9)=Y(IJK(9,I))
COORD(3,9)=Z(IJK(9,I))
DO 16 IC=1,3
DO 16 JC=1,9
COORDT(JC,IC)=COORD(IC,JC)
16 CONTINUE
DO 26 IC=1,9
DSQ(IC)=(COORD(1,IC)-CCPT(1))**2+(COORD(2,IC)-
A CCPT(2))**2+(COORD(3,IC)-CCPT(3))**2
DSQ(IC)=SQRT(DSQ(IC))
26 CONTINUE
INODE=0
IF (DSQ(1).LE.SMALL) INODE=1
IF (DSQ(2).LE.SMALL) INODE=2
IF (DSQ(3).LE.SMALL) INODE=3
IF (DSQ(4).LE.SMALL) INODE=4
IF (DSQ(5).LE.SMALL) INODE=5
IF (DSQ(6).LE.SMALL) INODE=6
IF (DSQ(7).LE.SMALL) INODE=7
IF (DSQ(8).LE.SMALL) INODE=8
IF (DSQ(9).LE.SMALL) INODE=9
IF (INODE.EQ.0) THEN
CALL RQINT(CCPT,G1,G1P,COORD,COORDT,IELTYPE(I))
ELSE
CALL SQINT(CCPT,G1,G1P,COORD,COORDT,INODE,IELTYPE(I))
END IF
END IF
DO 20 J=1,NS
AH1(IJK(J,I))=AH1(IJK(J,I))+G1P(J)
AH2(IJK(J,I))=AH2(IJK(J,I))+G1(J)
20 CONTINUE
10 CONTINUE
RETURN
END

C
C
C
SUBROUTINE RTINT(CCPT,G1,G1P,COORD,COORDT)
COMMON /VARS/ PI,INTFL
COMMON /QUAD/ SQPT,TQPT,WGT,GPT,SWGT
COMMON /TQUAD/ SGP(112,8),TGP(112,8),NSEV2(8),GWT(112,8)
DIMENSION CCPT(*),G1(*),G1P(*),COORD(3,9),COORDT(9,3)
DIMENSION SQPT(7),TQPT(7),WGT(7),GPT(4),SWGT(4)
DIMENSION DLH(2,6),DGH(2,3),RJ(2,2),QNORM(3)
DIMENSION UNORM(3),F(9),FP(9),CEN(3),DVEC(3)
DO 5 I=1,6
G1(I)=0.
G1P(I)=0.
5 CONTINUE

C DETERMINE SEVERITY
C
C FIND LONGEST SIDE OF TRIANGLE
C
S1=SQRT((COORD(1,2)-COORD(1,1))**2+(COORD(2,2)-
A COORD(2,1))**2+(COORD(3,2)-COORD(3,1))**2)
H=S1
S2=SQRT((COORD(1,3)-COORD(1,2))**2+(COORD(2,3)-
A COORD(2,2))**2+(COORD(3,3)-COORD(3,2))**2)

```

```

IF (S2.GT.H) H=S2
S3=SQRT((COORD(1,1)-COORD(1,3))**2+(COORD(2,1)-
A COORD(2,3))**2+(COORD(3,1)-COORD(3,3))**2)
IF (S3.GT.H) H=S3
DO 59 I=1,3
  A1=COORD(I,1)+COORD(I,2)+COORD(I,3)
  A2=COORD(I,4)+COORD(I,5)+COORD(I,6)
  CEN(I)=4.*A2/9.-A1/9.
59 CONTINUE
DVEC(1)=CCPT(1)-CEN(1)
DVEC(2)=CCPT(2)-CEN(2)
DVEC(3)=CCPT(3)-CEN(3)
D=SQRT(DVEC(1)**2+DVEC(2)**2+DVEC(3)**2)
HDD=H/D
IF (HDD.LT.0.358) THEN
  ISEV=1
ELSE
  CALL DER6T(1./3.,1./3.,DLH)
  DO 16 IC=1,2
  DO 16 JC=1,3
    SUM=0.0
    DO 36 KC=1,6
      SUM=SUM+DLH(IC,KC)*COORDT(KC,JC)
36   CONTINUE
    DGH(IC,JC)=SUM
16   CONTINUE
  QNORM(1)=DGH(1,2)*DGH(2,3)-DGH(1,3)*DGH(2,2)
  QNORM(2)=DGH(1,3)*DGH(2,1)-DGH(1,1)*DGH(2,3)
  QNORM(3)=DGH(1,1)*DGH(2,2)-DGH(1,2)*DGH(2,1)
  CALL UNORMAL(QNORM,UNORM)
  UDOTD=0.0
  DO 41 I=1,3
    UDOTD=UDOTD+UNORM(I)*DVEC(I)
41   CONTINUE
  COSTH=ABS(UDOTD/D)
  ISEV=(2.37+0.424*COSTH)*HDD+1
  IF (ISEV.GE.9) THEN
    WRITE(6,100) ISEV, (CCPT(I), I=1,3)
    ISEV=8
  ENDIF
ENDIF
100 FORMAT(' WARNING, SEVERITY NUMBER=',I2, ' AT CCPT= (',
A E10.4,' ,',E10.4,' ,',E10.4,' )'/' LARGE QUADRATURE
B ERRORS ARE POSSIBLE')
NO=NSEV2(ISEV)
DO 60 I=1,NO
  CALL DER6T(SGP(I,ISEV),TGP(I,ISEV),DLH)
  DO 15 IC=1,2
  DO 25 JC=1,3
    SUM=0.
    DO 35 KC=1,6
      SUM=SUM+DLH(IC,KC)*COORDT(KC,JC)
35   CONTINUE
    DGH(IC,JC)=SUM
25   CONTINUE
15   CONTINUE
  DO 50 IC=1,2
  DO 40 JC=1,2
    SUM=0.
    DO 30 KC=1,3
      SUM=SUM+DGH(IC,KC)*DGH(JC,KC)
30   CONTINUE
    RJ(IC,JC)=SUM
40   CONTINUE
50   CONTINUE
  DET2=RJ(1,1)*RJ(2,2)-RJ(1,2)*RJ(2,1)
  DETWT=SQRT(DET2)*GWT(I,ISEV)

```

```

QNORM(1)=DGH(1,2)*DGH(2,3)-DGH(1,3)*DGH(2,2)
QNORM(2)=DGH(1,3)*DGH(2,1)-DGH(1,1)*DGH(2,3)
QNORM(3)=DGH(1,1)*DGH(2,2)-DGH(1,2)*DGH(2,1)
CALL UNORMAL(QNORM,UNORM)
CALL FUNDS(SGP(I,ISEV),TGP(I,ISEV),COORD,CCPT,UNORM,F,FP,30)
DO 10 J=1,6
    G1(J)=G1(J)+F(J)*DETWT
    G1P(J)=G1P(J)+FP(J)*DETWT
10    CONTINUE
60    CONTINUE
    RETURN
    END

C
C
C
SUBROUTINE FUNDS(S,T,COORD,CCPT,UNORM,F,FP,IET)
DIMENSION COORD(3,9),CCPT(*),UNORM(*),H(9),F(9),FP(9)
DIMENSION QPT(3)
IF (IET.LT.40) THEN
    NS=6
C        IF (IET.EQ.30) THEN
C            CALL SHP6T(S,T,H)
C        ELSE
C            CALL SHP6TD(S,T,H)
C        ENDIF
C    ELSE
    NS=9
        IF (IET.EQ.40) THEN
            CALL SHP9T(S,T,H)
        ELSE
            CALL SHP9TD(S,T,H)
        ENDIF
    ENDIF
    DO 10 I=1,3
        QPT(I)=0.
    DO 10 J=1,NS
        QPT(I)=COORD(I,J)*H(J)+QPT(I)
10    CONTINUE
    R=SQRT((CCPT(1)-QPT(1))**2+(CCPT(2)-QPT(2))**2+(CCPT(3)-
A        QPT(3))**2)
    F1=(CCPT(1)-QPT(1))*UNORM(1)/R**3
    F2=(CCPT(2)-QPT(2))*UNORM(2)/R**3
    F3=(CCPT(3)-QPT(3))*UNORM(3)/R**3
    DO 20 I=1,NS
        FP(I)=(F1+F2+F3)*H(I)
        F(I)=H(I)/R
20    CONTINUE
    RETURN
    END

C
C
C
SUBROUTINE DER6T(S,T,DLH)
DIMENSION DLH(2,6)
DLH(1,1)=2.* (S+T-0.5)+2.* (S+T-1.)
DLH(1,2)=2.* (S-0.5)+2.* S
DLH(1,3)=0.
DLH(1,4)=-4.* (S+T-1.)-4.* S
DLH(1,5)=4.* T
DLH(1,6)=-4.* T
DLH(2,1)=DLH(1,1)
DLH(2,2)=0.
DLH(2,3)=2.* (T-0.5)+2.* T
DLH(2,4)=-4.* S
DLH(2,5)=4.* S
DLH(2,6)=-4.* (S+T-1.)-4.* T
RETURN

```

```

END
C
C
C
SUBROUTINE UNORMAL(Q,U)
COMMON /VARS/ PI,INTFL
DIMENSION Q(*),U(*)
F=1.
IF (INTFL.EQ.1) F=-1.
R=SQRT(Q(1)**2+Q(2)**2+Q(3)**2)
U(1)=F*Q(1)/R
U(2)=F*Q(2)/R
U(3)=F*Q(3)/R
RETURN
END
C
C
C
SUBROUTINE SHP6T(S,T,H)
DIMENSION H(9)
H(1)=2.* (S+T-0.5)*(S+T-1.)
H(2)=2.*S*(S-0.5)
H(3)=2.*T*(T-0.5)
H(4)=-4.*S*(S+T-1.)
H(5)=4.*S*T
H(6)=-4.*T*(S+T-1.)
RETURN
END
C
C
C
SUBROUTINE STINT(CCPT,G1,G1P,COORD,COORDT,INODE)
COMMON /VARS/ PI,INTFL
COMMON /QUAD/ SQPT,TQPT,WGT,GPT,SWGT
DIMENSION CCPT(*),G1(*),G1P(*),COORD(3,9),COORDT(9,3)
DIMENSION SQPT(7),TQPT(7),WGT(7),GPT(4),SWGT(4)
DIMENSION NODE(6),DLH(2,6),DGH(2,3),RJ(2,2)
DIMENSION NORDER(6,6),UNORM(3),QNORM(3),QPT(3)
DIMENSION F(9),FP(9),G1H(9),G1PH(9)
DATA NORDER/1,2,3,3,1,2,2,3,1,1,2,3,3,1,2,2,3,1,4,5,6
A      ,6,4,5,5,6,4,4,5,6,6,4,5,5,6,4/
DO 10 I=1,6
  NODE(I)=NORDER(INODE,I)
10 CONTINUE
DO 20 J=1,6
  NOD=NODE(J)
  DO 30 I=1,3
    COORDT(J,I)=COORD(I,NOD)
30 CONTINUE
20 CONTINUE
DO 40 I=1,3
  DO 40 J=1,6
    COORD(I,J)=COORDT(J,I)
40 CONTINUE
IF (INODE.LE.3) THEN
  INDX=1
  FACT=1.0
  A=0.0
  B=0.0
  C=1.0
ELSE
  INDX=2
  FACT=1.0/SQRT(2.)
  A=0.5
  B=-FACT
  C=-FACT
ENDIF

```

```

DO 50 I=1,6
  G1H(I)=0.
  G1PH(I)=0.
50 CONTINUE
DO 60 K=1,INDX
  TWOK=2*K
  SGN=3-TWOK
  DO 70 I=1,4
    PHI=(PI/4.)*(GPT(I)+TWOK-1.)
    SINPHI=SIN(PHI)
    COSPHI=COS(PHI)
    RHOUL=FACT/(SINPHI+SGN*COSPHI)
    WTI=RHOUL*SWGT(I)/2.
  DO 80 J=1,4
    RHO=(RHOUL/2.)*(GPT(J)+1.)
    S=A+RHO*(B*SINPHI+C*COSPHI)
    T=A+RHO*(C*SINPHI-B*COSPHI)
    CALL DER6T(S,T,DLH)
  DO 15 IC=1,2
  DO 25 JC=1,3
    SUM=0.
    DO 35 KC=1,6
      SUM=SUM+DLH(IC,KC)*COORDT(KC,JC)
35 CONTINUE
      DGH(IC,JC)=SUM
25 CONTINUE
15 CONTINUE
  DO 45 IC=1,2
  DO 55 JC=1,2
    SUM=0.
    DO 65 KC=1,3
      SUM=SUM+DGH(IC,KC)*DGH(JC,KC)
65 CONTINUE
      RJ(IC,JC)=SUM
55 CONTINUE
45 CONTINUE
  DET2=RJ(1,1)*RJ(2,2)-RJ(1,2)*RJ(2,1)
  WTJ=SQRT(DET2)*SWGT(J)*PI/4.
  QNORM(1)=DGH(1,2)*DGH(2,3)-DGH(1,3)*DGH(2,2)
  QNORM(2)=DGH(1,3)*DGH(2,1)-DGH(1,1)*DGH(2,3)
  QNORM(3)=DGH(1,1)*DGH(2,2)-DGH(1,2)*DGH(2,1)
  CALL UNORMAL(QNORM,UNORM)
  CALL FUNDS(S,T,COORD,CCPT,UNORM,F,FP,30)
  DO 75 J5=1,6
    G1H(J5)=G1H(J5)+WTJ*WTI*F(J5)*RHO
    G1PH(J5)=G1PH(J5)+WTJ*WTI*FP(J5)*RHO
75 CONTINUE
  DO 77 J6=1,6
    NOD=NORDER(INODE,J6)
    G1(NOD)=G1H(J6)
    G1P(NOD)=G1PH(J6)
77 CONTINUE
80 CONTINUE
70 CONTINUE
60 CONTINUE
  RETURN
END
C
C
C
SUBROUTINE RQINT(CCPT,G1,G1P,COORD,COORDT,IEL)
DIMENSION CCPT(*),G1(*),G1P(*),COORD(3,9),COORDT(9,3)
IF (IEL.LE.40) THEN
  CALL RQINTC(CCPT,G1,G1P,COORD,COORDT)
ELSE
  CALL RQINTD(CCPT,G1,G1P,COORD,COORDT,IEL)
ENDIF

```

```

RETURN
END
C
C
C
SUBROUTINE SQINT(CCPT,G1,G1P,COORD,COORDT,INODE,IEL)
COMMON /VARS/ PI,INTFL
DIMENSION CCPT(*),G1(*),G1P(*),COORD(3,9),COORDT(9,3)
DIMENSION ANG1(4),ANG2(4),FACT(4),IFL(4)
IF (INODE.LT.9) GO TO 10
  NTRI=4
  SOFF=0.
  TOFF=0.
  IFL(1)=1
  FACT(1)=1.
  ANG1(1)=-PI/4.
  ANG2(1)=PI/4.
  IFL(2)=2
  FACT(2)=1.
  ANG1(2)=PI/4.
  ANG2(2)=3.*PI/4.
  IFL(3)=1
  FACT(3)=-1.
  ANG1(3)=3.*PI/4.
  ANG2(3)=5.*PI/4.
  IFL(4)=2
  FACT(4)=-1.
  ANG1(4)=5.*PI/4.
  ANG2(4)=7.*PI/4.
  GO TO 150
10 CONTINUE
IF (INODE.LT.8) GO TO 20
  NTRI=3
  SOFF=-1.
  TOFF=0.
  IFL(1)=2
  FACT(1)=-1.
  ANG1(1)=3.*PI/2.
  ANG2(1)=2.*PI+ATAN2(-1.,2.)
  IFL(2)=1
  FACT(2)=2.
  ANG1(2)=-ATAN(0.5)
  ANG2(2)=ATAN(0.5)
  IFL(3)=2
  FACT(3)=1.
  ANG1(3)=ATAN(0.5)
  ANG2(3)=PI/2.
  GO TO 150
20 CONTINUE
IF (INODE.LT.7) GO TO 30
  NTRI=3
  SOFF=0.
  TOFF=1.
  IFL(1)=1
  FACT(1)=-1.
  ANG1(1)=PI
  ANG2(1)=2.*PI+ATAN2(-2.,-1.)
  IFL(2)=2
  FACT(2)=-2.
  ANG1(2)=2.*PI+ATAN2(-2.,-1.)
  ANG2(2)=2.*PI+ATAN2(-2.,1.)
  IFL(3)=1
  FACT(3)=1
  ANG1(3)=2.*PI+ATAN2(-2.,1.)
  ANG2(3)=2.*PI
  GO TO 150
30 CONTINUE

```

```

IF (INODE.LT.6) GO TO 40
  NTRI=3
  SOFF=1.
  TOFF=0.
  IFL(1)=2
  FACT(1)=1.
  ANG1(1)=PI/2.
  ANG2(1)=ATAN2(1.,-2.)
  IFL(2)=1
  FACT(2)=-2.
  ANG1(2)=ATAN2(1.,-2.)
  ANG2(2)=2.*PI+ATAN2(-1.,-2.)
  IFL(3)=2
  FACT(3)=-1.
  ANG1(3)=2.*PI+ATAN2(-1.,-2.)
  ANG2(3)=3.*PI/2.
  GO TO 150
40 CONTINUE
  IF (INODE.LT.5) GO TO 50
    IF (IEL.LE.40) THEN
      NTRI=3
      SOFF=0.
      TOFF=-1.
      IFL(1)=1
      FACT(1)=1.
      ANG1(1)=0.
      ANG2(1)=ATAN(2.)
      IFL(2)=2
      FACT(2)=2.
      ANG1(2)=ATAN(2.)
      ANG2(2)=ATAN2(2.,-1.)
      IFL(3)=1
      FACT(3)=-1.
      ANG1(3)=ATAN2(2.,-1.)
      ANG2(3)=PI
    ELSE
      NTRI=4
      SOFF=0.
      TOFF=-2./3.
      IFL(1)=2
      FACT(1)=-1./3.
      ANG1(1)=2.*PI+ATAN2(-1./3.,-1.)
      ANG2(1)=2.*PI+ATAN2(-1./3.,1.)
      IFL(2)=1
      FACT(2)=1.
      ANG1(2)=-ATAN(1./3.)
      ANG2(2)=ATAN(5./3.)
      IFL(3)=2
      FACT(3)=5./3.
      ANG1(3)=ATAN(5./3.)
      ANG2(3)=ATAN2(5./3.,-1.)
      IFL(4)=1
      FACT(4)=-1.
      ANG1(4)=ATAN2(5./3.,-1.)
      ANG2(4)=2.*PI+ATAN2(-1./3.,-1.)
    ENDIF
    GO TO 150
50 CONTINUE
  IF (INODE.LT.4) GO TO 60
    NTRI=2
    SOFF=-1.
    TOFF=1.
    IFL(1)=2
    FACT(1)=-2.
    ANG1(1)=3.*PI/2.
    ANG2(1)=7.*PI/4.
    IFL(2)=1

```

```

FACT(2)=2.
ANG1(2)=7.*PI/4.
ANG2(2)=2.*PI
GO TO 150
60 CONTINUE
IF (INODE.LT.3) GO TO 70
NTRI=2
SOFF=1.
TOFF=1.
IFL(1)=1
FACT(1)=-2.
ANG1(1)=PI
ANG2(1)=5.*PI/4.
IFL(2)=2
FACT(2)=-2.
ANG1(2)=5.*PI/4.
ANG2(2)=3.*PI/2.
GO TO 150
70 CONTINUE
IF (INODE.LT.2) GO TO 80
IF (IEL.LE.40) THEN
NTRI=2
SOFF=1.
TOFF=-1.
IFL(1)=2
FACT(1)=2.
ANG1(1)=PI/2.
ANG2(1)=3.*PI/4.
IFL(2)=1
FACT(2)=-2.
ANG1(2)=3.*PI/4.
ANG2(2)=PI
ELSE
NTRI=3
SOFF=1.
TOFF=-2./3.
ANG1(1)=PI/2.
ANG2(1)=ATAN2(5./3.,-2.)
IFL(1)=2
FACT(1)=5./3.
ANG1(2)=ATAN2(5./3.,-2.)
ANG2(2)=2.*PI+ATAN2(-1./3.,-2.)
IFL(2)=1
FACT(2)=-2.
ANG1(3)=2.*PI+ATAN2(-1./3.,-2.)
ANG2(3)=3.*PI/2.
IFL(3)=2
FACT(3)=-1./3.
ENDIF
GO TO 150
80 CONTINUE
IF (IEL.EQ.40) THEN
NTRI=2
SOFF=-1.
TOFF=-1.
ANG1(1)=0.
ANG2(1)=PI/4.
IFL(1)=1
FACT(1)=2.
ANG1(2)=PI/4.
ANG2(2)=PI/2.
IFL(2)=2
FACT(2)=2.
ELSE
NTRI=3
SOFF=-1.
TOFF=-2./3.

```



```

        IF (IEL.LE.40) THEN
            CALL DER9T(S,T,DLH)
        ELSE
            CALL DER9TD(S,T,DLH)
        ENDIF
        DO 15 IC=1,2
        DO 25 JC=1,3
            SUM=0.
            DO 35 KC=1,9
                SUM=SUM+DLH(IC,KC)*COORDT(KC,JC)
35            CONTINUE
                DGH(IC,JC)=SUM
25            CONTINUE
15            CONTINUE
            DO 45 IC=1,2
            DO 55 JC=1,2
                SUM=0.
                DO 65 KC=1,3
                    SUM=SUM+DGH(IC,KC)*DGH(JC,KC)
65            CONTINUE
                RJ(IC,JC)=SUM
55            CONTINUE
45            CONTINUE
DET2=RJ(1,1)*RJ(2,2)-RJ(1,2)*RJ(2,1)
WTJ=SQRT(DET2)*SWGT(J)*0.5*(ANG2(K)-ANG1(K))
QNORM(1)=DGH(1,2)*DGH(2,3)-DGH(1,3)*DGH(2,2)
QNORM(2)=DGH(1,3)*DGH(2,1)-DGH(1,1)*DGH(2,3)
QNORM(3)=DGH(1,1)*DGH(2,2)-DGH(1,2)*DGH(2,1)
CALL UNORMAL(QNORM,UNORM)
CALL FUNDS(S,T,COORD,CCPT,UNORM,F,FP,IEL)
DO 75 J5=1,9
    G1H(J5)=G1H(J5)+WTJ*WTI*F(J5)*RHO
    G1PH(J5)=G1PH(J5)+WTJ*WTI*FP(J5)*RHO
75            CONTINUE
    DO 77 J6=1,9
        IF (ISIDE.GT.1) THEN
            NOD=NORDER(ISIDE,J6)
        ELSE
            NOD=J6
        ENDIF
        G1(NOD)=G1H(J6)
        G1P(NOD)=G1PH(J6)
77            CONTINUE
80            CONTINUE
70            CONTINUE
60 CONTINUE
RETURN
END

C
C
C
SUBROUTINE RQINTC(CCPT,G1,G1P,COORD,COORDT)
COMMON /VARS/ PI,INTFL
COMMON /QUAD/ SQPT,TQPT,WGT,GPT,SWGT
COMMON /NQUAD/ GP(12,8),GW(12,8),NSEV(8)
DIMENSION CCPT(*),G1(*),G1P(*),COORD(3,9),COORDT(9,3)
DIMENSION SQPT(7),TQPT(7),WGT(7),GPT(4),SWGT(4)
DIMENSION DLH(2,9),DGH(2,3),RJ(2,2),QNORM(3)
DIMENSION UNORM(3),F(9),FP(9),DVEC(3)
DO 5 I=1,9
    G1(I)=0.
    G1P(I)=0.
5 CONTINUE

C
C DETERMINE SEVERITY
C
C FIND LONGEST DIAGONAL OF ELEMENT

```

```

C
      D1=SQRT((COORD(1,3)-COORD(1,1))**2+(COORD(2,3)-COORD(2,1))**2+
A          (COORD(3,3)-COORD(3,1))**2)
      H=D1
      D2=SQRT((COORD(1,4)-COORD(1,2))**2+(COORD(2,4)-COORD(2,2))**2+
A          (COORD(3,4)-COORD(3,2))**2)
      IF (D2.GT.H) H=D2
      DVEC(1)=CCPT(1)-COORD(1,9)
      DVEC(2)=CCPT(2)-COORD(2,9)
      DVEC(3)=CCPT(3)-COORD(3,9)
      D=SQRT(DVEC(1)**2+DVEC(2)**2+DVEC(3)**2)
      HDD=H/D
      IF (HDD.LT.0.358) THEN
          ISEV=1
      ELSE
          CALL DER9T(0.,0.,DLH)
          DO 16 IC=1,2
              DO 16 JC=1,3
                  SUM=0.0
                  DO 36 KC=1,9
                      SUM=SUM+DLH(IC,KC)*COORDT(KC,JC)
36          CONTINUE
          DGH(IC,JC)=SUM
16          CONTINUE
          QNORM(1)=DGH(1,2)*DGH(2,3)-DGH(1,3)*DGH(2,2)
          QNORM(2)=DGH(1,3)*DGH(2,1)-DGH(1,1)*DGH(2,3)
          QNORM(3)=DGH(1,1)*DGH(2,2)-DGH(1,2)*DGH(2,1)
          CALL UNORMAL(QNORM,UNORM)
          UDOTD=0.0
          DO 41 I=1,3
              UDOTD=UDOTD+UNORM(I)*DVEC(I)
41          CONTINUE
          COSTH=ABS(UDOTD/D)
          ISEV=(2.37+0.424*COSTH)*HDD+1
          IF (ISEV.GE.9) THEN
              WRITE(6,100) ISEV, (CCPT(I), I=1,3)
              ISEV=8
          ENDIF
      ENDIF
100 FORMAT(' WARNING, SEVERITY NUMBER = (',I2,' AT
A CCPT=' ,E10.4,' ,',E10.4,' ,',E10.4,' )' /' LARGE
B QUADRATURE ERRORS ARE POSSIBLE' /)
      NQ=NSEV(ISEV)
      DO 60 I=1,NQ
      DO 60 J=1,NQ
          CALL DER9T(GP(I,ISEV),GP(J,ISEV),DLH)
          DO 15 IC=1,2
          DO 25 JC=1,3
              SUM=0.0
              DO 35 KC=1,9
                  SUM=SUM+DLH(IC,KC)*COORDT(KC,JC)
35          CONTINUE
          DGH(IC,JC)=SUM
25          CONTINUE
15          CONTINUE
          DO 50 IC=1,2
          DO 40 JC=1,2
              SUM=0.0
              DO 30 KC=1,3
                  SUM=SUM+DGH(IC,KC)*DGH(JC,KC)
30          CONTINUE
          RJ(IC,JC)=SUM
40          CONTINUE
50          CONTINUE
          DET2=RJ(1,1)*RJ(2,2)-RJ(1,2)*RJ(2,1)
          DETWT=SQRT(DET2)*GW(I,ISEV)*GW(J,ISEV)
          QNORM(1)=DGH(1,2)*DGH(2,3)-DGH(1,3)*DGH(2,2)

```

```

QNORM(2)=DGH(1,3)*DGH(2,1)-DGH(1,1)*DGH(2,3)
QNORM(3)=DGH(1,1)*DGH(2,2)-DGH(1,2)*DGH(2,1)
CALL UNORMAL(QNORM,UNORM)
CALL FUNDS(GP(I,ISEV),GP(J,ISEV),COORD,CCPT,UNORM,F,FP,40)
DO 10 J2=1,9
    G1(J2)=G1(J2)+F(J2)*DETWT
    G1P(J2)=G1P(J2)+FP(J2)*DETWT
10    CONTINUE
60    CONTINUE
    RETURN
    END
C
C
C
SUBROUTINE RQINTD(CCPT,G1,G1P,COORD,COORDT,IEL)
COMMON /VARS/ PI,INTFL
COMMON /QUAD/ SQPT,TQPT,WGT,GPT,SWGT
DIMENSION CCPT(*),G1(*),G1P(*),COORD(3,9),COORDT(9,3)
DIMENSION SQPT(7),TQPT(7),WGT(7),GPT(4),SWGT(4)
DIMENSION DLH(2,9),DGH(2,3),RJ(2,2),QNORM(3)
DIMENSION G1H(9),G1PH(9)
DIMENSION UNORM(3),F(9),FP(9),NORDER(4,9),NODE(9)
DATA NORDER/1,2,3,4,2,3,4,1,3,4,1,2,4,1,2,3,5,6,7,8,6,7,
A           8,5,7,8,5,6,8,5,6,7,9,9,9,9/
ISIDE=IEL-40
DO 11 I=1,9
    NODE(I)=NORDER(ISIDE,I)
11    CONTINUE
DO 21 J=1,9
    NOD=NODE(J)
    DO 31 I=1,3
        COORDT(J,I)=COORD(I,NOD)
31    CONTINUE
21    CONTINUE
    DO 41 I=1,3
    DO 41 J=1,9
        COORD(I,J)=COORDT(J,I)
41    CONTINUE
    DO 5  I=1,9
        G1H(I)=0.
        G1PH(I)=0.
5    CONTINUE
    DO 60 I=1,4
    DO 60 J=1,4
        CALL DER9TD(GPT(I),GPT(J),DLH)
        DO 15 IC=1,2
        DO 25 JC=1,3
            SUM=0.0
            DO 35 KC=1,9
                SUM=SUM+DLH(IC,KC)*COORDT(KC,JC)
35    CONTINUE
        DGH(IC,JC)=SUM
25    CONTINUE
15    CONTINUE
        DO 50 IC=1,2
        DO 40 JC=1,2
            SUM=0.0
            DO 30 KC=1,3
                SUM=SUM+DGH(IC,KC)*DGH(JC,KC)
30    CONTINUE
        RJ(IC,JC)=SUM
40    CONTINUE
50    CONTINUE
DET2=RJ(1,1)*RJ(2,2)-RJ(1,2)*RJ(2,1)
DETWT=SQRT(DET2)*SWGT(I)*SWGT(J)
QNORM(1)=DGH(1,2)*DGH(2,3)-DGH(1,3)*DGH(2,2)
QNORM(2)=DGH(1,3)*DGH(2,1)-DGH(1,1)*DGH(2,3)

```

```

QNORM(3)=DGH(1,1)*DGH(2,2)-DGH(1,2)*DGH(2,1)
CALL UNORMAL(QNORM,UNORM)
CALL FUNDS(GPT(I),GPT(J),COORD,CCPT,UNORM,F,FP,41)
DO 10 J2=1,9
    G1H(J2)=G1H(J2)+F(J2)*DETWT
    G1PH(J2)=G1PH(J2)+FP(J2)*DETWT
10  CONTINUE
    DO 77 J6=1,9
        NOD=NORDER(ISIDE,J6)
        G1(NOD)=G1H(J6)
        G1P(NOD)=G1PH(J6)
77  CONTINUE
60  CONTINUE
    RETURN
    END

C
C
C
SUBROUTINE GEOM(X,Y,Z,IJK,NODES,NE,PHI,PHIP,BET,GAM,IELTYPE,
A          NBDY,ICFL,XACP,YACP,ZACP)
COMMON /VARS/ PI,INTFL
CHARACTER TITLE1*80,TITLE2*80,TITLE3*80
DIMENSION X(*),Y(*),Z(*),IJK(9,1),UN(4001,20,3)
DIMENSION PHIP(*),IELTYPE(*),ICON(4001),PHI(*),BET(*)
DIMENSION S(9),T(9),SS(6),TT(6),COORDT(9,3),DLHT(2,6)
DIMENSION DLH(2,9),DGH(2,3),QNORM(3),UNORM(3),GAM(*)
DIMENSION NBDY(*),ICFL(*),XACP(*),YACP(*),ZACP(*)
READ(5,100) TITLE1
READ(5,100) TITLE2
READ(5,100) TITLE3
WRITE(6,101) TITLE1
WRITE(6,101) TITLE2
WRITE(6,101) TITLE3
100 FORMAT(A)
101 FORMAT(1X,A)
    READ(5,*) INTFL,IEXTRA
    DATA S/-1.,1.,1.,-1.,0.,1.,0.,-1.,0./
    DATA T/-1.,-1.,1.,1.,-1.,0.,1.,0.,0./
    DATA SS/0.,1.,0.,0.5,0.5,0./
    DATA TT/0.,0.,1.,0.,0.5,0.5/
    READ(5,*) NODES,NE
    DO 10 I=1,NODES
        ICON(I)=0
        READ(5,*) NI,X(NI),Y(NI),Z(NI),PAR1,PAR2,NBDY(NI),
A          ICFL(NI)
        IF (NBDY(NI).EQ.1) THEN
            PHI(NI)=PAR1
        ELSE
            IF (NBDY(NI).EQ.2) THEN
                PHIP(NI)=PAR1
            ELSE
                BET(NI)=PAR1
                GAM(NI)=PAR2
            ENDIF
        ENDIF
10  CONTINUE
    DO 20 I=1,NE
        READ(5,*) NI,IELTYPE(NI),(IJK(J,NI),J=1,9)
20  CONTINUE
    DO 30 I=1,IEXTRA
        READ(5,*) XACP(I),YACP(I),ZACP(I)
30  CONTINUE
    RETURN
    END

```

```

SUBROUTINE CALPHI(X,Y,Z,IJK,NODES,NE,B,PHI,PHIP,BET,GAM,
A      IELTYPE,NBDY)
COMMON /VARS/ PI,INTFL
COMMON /QUAD/ SQPT,TQPT,WGT,GPT,SWGT
DIMENSION X(*),Y(*),Z(*),IJK(9,1),B(*),IELTYPE(*)
DIMENSION SQPT(7),TQPT(7),WGT(7),GPT(4),SWGT(4)
DIMENSION AH1(4001),AH2(4001),CCPT(3),PHIP(*)
DIMENSION PHI(*),BET(*),GAM(*),NBDY(*)
READ(5,*) INUM
IF (INUM.EQ.0) GO TO 30
WRITE(6,100)
100 FORMAT(//10X,' SOLUTION VALUES AT SELECTED POINTS')
DO 10 I=1,INUM
    READ(5,*) CCPT(1),CCPT(2),CCPT(3)
    CALL INT4(0,CCPT,AH1,AH2,NODES,NE,IJK,X,Y,Z,IELTYPE)
    PS=0.
    DO 20 J=1,NODES
        GO TO (41,51,61) NBDY(J)
41     CONTINUE
        PS=PS-PHI(J)*AH1(J)+B(J)*AH2(J)
        GO TO 20
51     CONTINUE
        PS=PS-B(J)*AH1(J)+PHIP(J)*AH2(J)
        GO TO 20
61     CONTINUE
        PHI(J)=GAM(J)-BET(J)*B(J)
        PS=PS-PHI(J)*AH1(J)+B(J)*AH2(J)
20     CONTINUE
        PS=PS/(4.*PI)
        PSE=CCPT(1)+2.*CCPT(1)*CCPT(2)-CCPT(2)+CCPT(1)*
A      CCPT(2)*CCPT(3)
        WRITE(6,200) CCPT(1),CCPT(2),CCPT(3),PS,PSE
10     CONTINUE
30     CONTINUE
200    FORMAT(' X=',F9.4,2X,'Y=',F9.4,2X,'Z=',F9.4,
A      2X,'PHI=',E14.6,2X,'X=',E14.6)
      RETURN
      END
C
C
C
      SUBROUTINE DECOMP(N,COND,IPVT,WORK,A)
      DIMENSION IPVT(*),WORK(*),A(4001,4001)
      IPVT(N)=1
      IF(N .EQ. 1) GO TO 80
      NM1=N-1
      ANORM=0.0
      DO 10 J=1,N
      T=0.0
      DO 5 I=1,N
      T=T+ABS(A(I,J))
5       CONTINUE
      IF(T .GT. ANORM) ANORM=T
10     CONTINUE
      DO 35 K=1,NM1
      KP1=K+1
      M=K
      DO 15 I=KP1,N
      IF(ABS(A(I,K)) .GT. ABS(A(M,K))) M=I
15     CONTINUE
      IPVT(K)=M
      IF( M .NE. K ) IPVT(N)=-IPVT(N)
      T=A(M,K)
      A(M,K)=A(K,K)
      A(K,K)=T
      IF(T .EQ. 0.0) GO TO 35
      DO 20 I=KP1,N

```

```

20      A(I,K)=-A(I,K)/T
CONTINUE
DO 30 J=KP1,N
T=A(M,J)
A(M,J)=A(K,J)
A(K,J)=T
IF( T .EQ. 0.0 ) GO TO 30
DO 25 I=KP1,N
A(I,J)=A(I,J)+A(I,K)*T
25      CONTINUE
30      CONTINUE
35      CONTINUE
DO 50 K=1,N
T=0.0
IF(K .EQ. 1) GO TO 45
KM1=K-1
DO 40 I=1,KM1
T=T+A(I,K)*WORK(I)
40      CONTINUE
45      EK=1.0
IF(T .LT. 0.0) EK=-1
IF(A(K,K) .EQ. 0.0) GO TO 90
WORK(K)=- (EK+T)/A(K,K)
50      CONTINUE
DO 60 KB=1,NM1
K=N-KB
T=0.0
KP1=K+1
DO 55 I=KP1,N
T=T+A(I,K)*WORK(K)
55      CONTINUE
WORK(K)=T
M=IPVT(K)
IF(M .EQ. K) GO TO 60
T=WORK(M)
WORK(M)=WORK(K)
WORK(K)=T
60      CONTINUE
YNORM=0.0
DO 65 I=1,N
YNORM=YNORM+ABS(WORK(I))
65      CONTINUE
CALL SOLVE(N,WORK,IPVT,A)
ZNORM=0.0
DO 70 I=1,N
ZNORM=ZNORM+ABS(WORK(I))
70      CONTINUE
COND=ANORM*ZNORM/YNORM
IF(COND .LT. 1.0) COND=1.0
RETURN
80      COND=1.0
IF(A(1,1) .NE. 0.0) RETURN
COND=1.0D+32
RETURN
END
C
C
C
SUBROUTINE SOLVE(N,B,IPVT,A)
DIMENSION B(*),IPVT(*),A(4001,4001)
IF( N .EQ. 1) GO TO 50
NM1=N-1
DO 20 K=1,NM1
KP1=K+1
M=IPVT(K)
T=B(M)
B(M)=B(K)

```

```

      B(K)=T
      DO 10 I=KP1,N
      B(I)=B(I)+A(I,K)*T
10      CONTINUE
20      CONTINUE
      DO 40 KB=1,NM1
      KM1=N-KB
      K=KM1+1
      B(K)=B(K)/A(K,K)
      T=-B(K)
      DO 30 I=1,KM1
      B(I)=B(I)+A(I,K)*T
30      CONTINUE
40      CONTINUE
50      B(1)=B(1)/A(1,1)
      RETURN
      END

C
C
C

      SUBROUTINE DER9TD(S,T,DLH)
      DIMENSION DLH(2,9)
      DLH(1,1)=9.*(2.*S*T**2-2.*S*T-T**2+T)/20.
      DLH(1,2)=9.*(2.*S*T**2-2.*S*T+T**2-T)/20.
      DLH(1,3)=3.*(2.*S*T**2+4.*S*T/3.+T**2+2.*T/3.)/10.
      DLH(1,4)=3.*(2.*S*T**2+4.*S*T/3.-T**2-2.*T/3.)/10.
      DLH(1,5)=-9.*(2.*S*T**2-2.*S*T)/10.
      DLH(1,6)=-3.*(2.*S*T**2-2.*S*T/3.-4.*S/3.+T**2-
A          T/3.-2./3.)/4.
      DLH(1,7)=-3.*(2.*S*T**2+4.*S*T/3.)/5.
      DLH(1,8)=-3.*(2.*S*T**2-2.*S*T/3.-4.*S/3.-T**2+
A          T/3.+2./3.)/4.
      DLH(1,9)=3.*(2.*S*T**2-2.*S*T/3.-4.*S/3.)/2.
      DLH(2,1)=9.*(2.*S**2*T-S**2-2.*S*T+S)/20.
      DLH(2,2)=9.*(2.*S**2*T-S**2+2.*S*T-S)/20.
      DLH(2,3)=3.*(2.*S**2*T+2.*S**2/3.+2.*S*T+2.*S/3.)/10.
      DLH(2,4)=3.*(2.*S**2*T+2.*S**2/3.-2.*S*T-2.*S/3.)/10.
      DLH(2,5)=-9.*(2.*S**2*T-S**2-2.*T+1.)/10.
      DLH(2,6)=-3.*(2.*S**2*T-S**2/3.+2.*S*T-S/3.)/4.
      DLH(2,7)=-3.*(2.*S**2*T+2.*S**2/3.-2.*T-2./3.)/5.
      DLH(2,8)=-3.*(2.*S**2*T-S**2/3.-2.*S*T+S/3.)/4.
      DLH(2,9)=3.*(2.*S**2*T-S**2/3.-2.*T+1./3.)/2.
      RETURN
      END

C
C
C

      SUBROUTINE DER9T(S,T,DLHQ)
      DIMENSION DLHQ(2,9)
      DLHQ(1,1)=0.250*(2.0*S*T**2-2.0*S*T-T**2+T)
      DLHQ(1,2)=0.250*(2.0*S*T**2-2.0*S*T+T**2-T)
      DLHQ(1,3)=0.250*(2.0*S*T**2+2.0*S*T+T**2+T)
      DLHQ(1,4)=0.250*(2.0*S*T**2+2.0*S*T-T**2-T)
      DLHQ(1,5)=-0.50*(2.0*S*T**2-2.0*S*T)
      DLHQ(1,6)=-0.50*(2.0*S*T**2+T**2-2.0*S-1.0)
      DLHQ(1,7)=-0.50*(2.0*S*T**2+2.0*S*T)
      DLHQ(1,8)=-0.50*(2.0*S*T**2-T**2-2.0*S+1.0)
      DLHQ(1,9)=2.0*S*T**2-2.0*S
      DLHQ(2,1)=0.250*(2.0*S**2*T-S**2-2.0*S*T+S)
      DLHQ(2,2)=0.250*(2.0*S**2*T-S**2+2.0*S*T-S)
      DLHQ(2,3)=0.250*(2.0*S**2*T+S**2+2.0*S*T+S)
      DLHQ(2,4)=0.250*(2.0*S**2*T+S**2-2.0*S*T-S)
      DLHQ(2,5)=-0.50*(2.0*S**2*T-S**2-2.0*T+1.0)
      DLHQ(2,6)=-0.50*(2.0*S**2*T+2.0*S*T)
      DLHQ(2,7)=-0.50*(2.0*S**2*T+S**2-2.0*T-1.0)
      DLHQ(2,8)=-0.50*(2.0*S**2*T-2.0*S*T)
      DLHQ(2,9)=2.0*S**2*T-2.0*T

```

```

RETURN
END
C
C
C
SUBROUTINE SHP9T(S,T,H)
DIMENSION H(9)
H(1)=S*T*(S-1.0)*(T-1.0)/4.0
H(2)=S*T*(S+1.0)*(T-1.0)/4.0
H(3)=S*T*(S+1.0)*(T+1.0)/4.0
H(4)=S*T*(S-1.0)*(T+1.0)/4.0
H(5)=-0.50*T*(S+1.0)*(S-1.0)*(T-1.0)
H(6)=-0.50*S*(T+1.0)*(T-1.0)*(S+1.0)
H(7)=-0.50*T*(S+1.0)*(S-1.0)*(T+1.0)
H(8)=-0.50*S*(T+1.0)*(T-1.0)*(S-1.0)
H(9)=(S+1.0)*(S-1.0)*(T+1.0)*(T-1.0)
RETURN
END
C
C
C
SUBROUTINE SHP9TD(S,T,H)
DIMENSION H(9)
H(1)=9.*S*T*(S-1.)*(T-1.)/20.
H(2)=9.*S*T*(S+1.)*(T-1.)/20.
H(3)=3.*S*T*(S+1.)*(T+2./3.)/10.
H(4)=3.*S*T*(S-1.)*(T+2./3.)/10.
H(5)=-9.*T*(S+1.)*(S-1.)*(T-1.)/10.
H(6)=-3.*S*(T-1.)*(T+2./3.)*(S+1.)/4.
H(7)=-3.*T*(S+1.)*(S-1.)*(T+2./3.)/5.
H(8)=-3.*S*(T-1.)*(T+2./3.)*(S-1.)/4.
H(9)=1.5*(S+1.)*(S-1.)*(T+2./3.)*(T-1.)
RETURN
END
C
C
C
SUBROUTINE QUADR
COMMON /NQUAD/ GP(12,8),GW(12,8),NSEV(8)
COMMON /TQUAD/ SGP(112,8),TGP(112,8),NSEV2(8),GWT(112,8)
NSEV(1)=2
NSEV(2)=3
NSEV(3)=4
NSEV(4)=5
NSEV(5)=6
NSEV(6)=8
NSEV(7)=10
NSEV(8)=12
GP(1,1)=-0.577350269189626
GP(2,1)=-GP(1,1)
GW(1,1)=1.0
GW(2,1)=1.0
GP(1,2)=-0.774596669241483
GP(2,2)=0.0
GP(3,2)=-GP(1,2)
GW(1,2)=0.5555555555555556
GW(2,2)=0.8888888888888889
GW(3,2)=GW(1,2)
GP(1,3)=-0.861136311594053
GP(2,3)=-0.339981043584856
GP(3,3)=-GP(2,3)
GP(4,3)=-GP(1,3)
GW(1,3)=0.347854845137454
GW(2,3)=0.652145154862546
GW(3,3)=GW(2,3)
GW(4,3)=GW(1,3)
GP(1,4)=-0.906179845938664

```

```

GP(2,4)=-0.538469310105683
GP(3,4)=0.0
GP(4,4)=-GP(2,4)
GP(5,4)=-GP(1,4)
GW(1,4)=0.236926885056189
GW(2,4)=0.478628670499366
GW(3,4)=0.568888888888889
GW(4,4)=GW(2,4)
GW(5,4)=GW(1,4)
GP(1,5)=-0.932469514203152
GP(2,5)=-0.661209384666265
GP(3,5)=-0.238619186083197
GP(4,5)=-GP(3,5)
GP(5,5)=-GP(2,5)
GP(6,5)=-GP(1,5)
GW(1,5)=0.171324492379170
GW(2,5)=0.360761573048139
GW(3,5)=0.467913934572691
GW(4,5)=GW(3,5)
GW(5,5)=GW(2,5)
GW(6,5)=GW(1,5)
GP(1,6)=-0.960289856497536
GP(2,6)=-0.796666477413627
GP(3,6)=-0.525532409916329
GP(4,6)=-0.183434642495650
GP(5,6)=-GP(4,6)
GP(6,6)=-GP(3,6)
GP(7,6)=-GP(2,6)
GP(8,6)=-GP(1,6)
GW(1,6)=0.101228536290376
GW(2,6)=0.222381034453374
GW(3,6)=0.313706645877887
GW(4,6)=0.362683788378362
GW(5,6)=GW(4,6)
GW(6,6)=GW(3,6)
GW(7,6)=GW(2,6)
GW(8,6)=GW(1,6)
GP(1,7)=-0.973906528517172
GP(2,7)=-0.865063366688985
GP(3,7)=-0.679409568299024
GP(4,7)=-0.433395394129247
GP(5,7)=-0.148874338981631
GP(6,7)=-GP(5,7)
GP(7,7)=-GP(4,7)
GP(8,7)=-GP(3,7)
GP(9,7)=-GP(2,7)
GP(10,7)=-GP(1,7)
GW(1,7)=0.066671344308668
GW(2,7)=0.149451349150581
GW(3,7)=0.219086362515982
GW(4,7)=0.269266719309996
GW(5,7)=0.295524224714753
GW(6,7)=GW(5,7)
GW(7,7)=GW(4,7)
GW(8,7)=GW(3,7)
GW(9,7)=GW(2,7)
GW(10,7)=GW(1,7)
GP(1,8)=-0.981560634246719
GP(2,8)=-0.904117256370475
GP(3,8)=-0.769902674194305
GP(4,8)=-0.587317954286617
GP(5,8)=-0.367831498998180
GP(6,8)=-0.125233408511469
GP(7,8)=-GP(6,8)
GP(8,8)=-GP(5,8)
GP(9,8)=-GP(4,8)
GP(10,8)=-GP(3,8)

```

```

GP(11,8)=-GP(2,8)
GP(12,8)=-GP(1,8)
GW(1,8)=0.047175336386512
GW(2,8)=0.106939325995318
GW(3,8)=0.160078328543346
GW(4,8)=0.203167426723066
GW(5,8)=0.233492536538355
GW(6,8)=0.249147045813403
GW(7,8)=GW(6,8)
GW(8,8)=GW(5,8)
GW(9,8)=GW(4,8)
GW(10,8)=GW(3,8)
GW(11,8)=GW(2,8)
GW(12,8)=GW(1,8)
NSEV2(1)=6
NSEV2(2)=7
NSEV2(3)=16
NSEV2(4)=19
NSEV2(5)=28
NSEV2(6)=64
NSEV2(7)=76
NSEV2(8)=112
SGP(1,1)=0.9157621/10.
SGP(2,1)=SGP(1,1)
SGP(3,1)=0.8168476
SGP(4,1)= 0.4459485
SGP(5,1)=SGP(4,1)
SGP(6,1)=0.1081030
TGP(1,1)=SGP(1,1)
TGP(2,1)=0.8168476
TGP(3,1)=0.9157621/10.
TGP(4,1)=SGP(4,1)
TGP(5,1)=SGP(6,1)
TGP(6,1)=SGP(4,1)
FACT=SQRT(3.)/2.
GWT(1,1)=FACT*0.6348067/10.
GWT(2,1)=GWT(1,1)
GWT(3,1)=GWT(1,1)
GWT(4,1)=FACT*0.1289694
GWT(5,1)=GWT(4,1)
GWT(6,1)=GWT(5,1)
SGP(1,2)=1./3.
SGP(2,2)=0.1012865
SGP(3,2)=SGP(2,2)
SGP(4,2)=0.7974270
SGP(5,2)=0.4701421
SGP(6,2)=SGP(5,2)
SGP(7,2)=0.5971587/10.
TGP(1,2)=SGP(1,2)
TGP(2,2)=SGP(2,2)
TGP(3,2)=0.7974270
TGP(4,2)=SGP(2,2)
TGP(5,2)=SGP(5,2)
TGP(6,2)=SGP(7,2)
TGP(7,2)=SGP(5,2)
GWT(1,2)=0.1125
GWT(2,2)=FACT*0.7271102/10.
GWT(3,2)=GWT(2,2)
GWT(4,2)=GWT(2,2)
GWT(5,2)=FACT*0.7643780/10.
GWT(6,2)=GWT(5,2)
GWT(7,2)=GWT(5,2)
SGP(1,3)=1./3.
TGP(1,3)=1./3.
SGP(2,3)=0.4592926
TGP(2,3)=SGP(2,3)
SGP(3,3)=SGP(2,3)

```

```

TGP(3,3)=0.8141482/10.
SGP(4,3)=TGP(3,3)
TGP(4,3)=SGP(2,3)
SGP(5,3)=0.5054723/10.
TGP(5,3)=SGP(5,3)
SGP(6,3)=SGP(5,3)
TGP(6,3)=0.8989055
SGP(7,3)=TGP(6,3)
TGP(7,3)=SGP(5,3)
SGP(8,3)=0.1705693
TGP(8,3)=SGP(8,3)
SGP(9,3)=SGP(8,3)
TGP(9,3)=0.6588614
SGP(10,3)=TGP(9,3)
TGP(10,3)=SGP(8,3)
SGP(11,3)=0.7284924
TGP(11,3)=0.2631128
SGP(12,3)=TGP(11,3)
TGP(12,3)=SGP(11,3)
SGP(13,3)=0.8394777/100.
TGP(13,3)=TGP(11,3)
SGP(14,3)=TGP(11,3)
TGP(14,3)=SGP(13,3)
SGP(15,3)=SGP(13,3)
TGP(15,3)=SGP(11,3)
SGP(16,3)=SGP(11,3)
TGP(16,3)=SGP(13,3)
GWT(1,3)=FACT*0.8332066/10.
DO 10 I=2,4
      GWT(I,3)=FACT*0.5490118/10.
10 CONTINUE
DO 11 I=5,7
      GWT(I,3)=FACT*0.1873992/10.
11 CONTINUE
DO 12 I=8,10
      GWT(I,3)=FACT*0.5959258/10.
12 CONTINUE
DO 13 I=11,16
      GWT(I,3)=FACT*0.1572143/10.
13 CONTINUE
SGP(1,4)=1./3.
TGP(1,4)=1./3.
SGP(2,4)=0.4896825
TGP(2,4)=SGP(2,4)
SGP(3,4)=SGP(2,4)
TGP(3,4)=0.2063496/10.
SGP(4,4)=TGP(3,4)
TGP(4,4)=SGP(2,4)
SGP(5,4)=0.4370896
TGP(5,4)=SGP(5,4)
SGP(6,4)=SGP(5,4)
TGP(6,4)=0.1258208
SGP(7,4)=TGP(6,4)
TGP(7,4)=SGP(5,4)
SGP(8,4)=0.1882035
TGP(8,4)=SGP(8,4)
SGP(9,4)=SGP(8,4)
TGP(9,4)=0.6235929
SGP(10,4)=TGP(9,4)
TGP(10,4)=SGP(9,4)
SGP(11,4)=0.4472951/10.
TGP(11,4)=SGP(11,4)
SGP(12,4)=SGP(11,4)
TGP(12,4)=0.9105410
SGP(13,4)=TGP(12,4)
TGP(13,4)=SGP(11,4)
SGP(14,4)=0.7411986

```

```

TGP(14,4)=0.2219630
SGP(15,4)=TGP(14,4)
TGP(15,4)=SGP(14,4)
SGP(16,4)=0.3683841/10.
TGP(16,4)=TGP(14,4)
SGP(17,4)=TGP(14,4)
TGP(17,4)=SGP(16,4)
SGP(18,4)=SGP(16,4)
TGP(18,4)=SGP(14,4)
SGP(19,4)=SGP(14,4)
TGP(19,4)=SGP(16,4)
GWT(1,4)=FACT*0.5608138/10.
DO 21 I=2,4
    GWT(I,4)=FACT*0.1809110/10.
21 CONTINUE
DO 22 I=5,7
    GWT(I,4)=FACT*0.4493375/10.
22 CONTINUE
DO 23 I=8,10
    GWT(I,4)=FACT*0.4598464/10.
23 CONTINUE
DO 24 I=11,13
    GWT(I,4)=FACT*0.1476728/10.
24 CONTINUE
DO 25 I=14,19
    GWT(I,4)=FACT*0.2498976/10.
25 CONTINUE
SGP(1,5)=1./3.
TGP(1,5)=1./3.
SGP(2,5)=0.2598914/10.
TGP(2,5)=SGP(2,5)
SGP(3,5)=SGP(2,5)
TGP(3,5)=0.9480217
SGP(4,5)=TGP(3,5)
TGP(4,5)=SGP(2,5)
SGP(5,5)=0.9428750/10.
TGP(5,5)=SGP(5,5)
SGP(6,5)=SGP(5,5)
TGP(6,5)=0.8114250
SGP(7,5)=TGP(6,5)
TGP(7,5)=SGP(5,5)
SGP(8,5)=0.4946368
TGP(8,5)=SGP(8,5)
SGP(9,5)=SGP(8,5)
TGP(9,5)=0.1072645/10.
SGP(10,5)=TGP(9,5)
TGP(10,5)=SGP(8,5)
SGP(11,5)=0.2073434
TGP(11,5)=SGP(11,5)
SGP(12,5)=SGP(11,5)
TGP(12,5)=0.5853132
SGP(13,5)=TGP(12,5)
TGP(13,5)=SGP(11,5)
SGP(14,5)=0.4389078
TGP(14,5)=SGP(14,5)
SGP(15,5)=SGP(14,5)
TGP(15,5)=0.1221844
SGP(16,5)=TGP(15,5)
TGP(16,5)=SGP(14,5)
SGP(17,5)=0.8588703
TGP(17,5)=0.1411297
SGP(18,5)=TGP(17,5)
TGP(18,5)=SGP(17,5)
SGP(19,5)=0.
TGP(19,5)=TGP(17,5)
SGP(20,5)=TGP(17,5)
TGP(20,5)=0.

```

```

SGP(21,5)=0.
TGP(21,5)=SGP(17,5)
SGP(22,5)=SGP(17,5)
TGP(22,5)=0.
SGP(23,5)=0.6779377
TGP(23,5)=0.2772206
SGP(24,5)=TGP(23,5)
TGP(24,5)=SGP(23,5)
SGP(25,5)=0.4484168/10.
TGP(25,5)=TGP(23,5)
SGP(26,5)=TGP(23,5)
TGP(26,5)=SGP(25,5)
SGP(27,5)=SGP(25,5)
TGP(27,5)=SGP(23,5)
SGP(28,5)=SGP(23,5)
TGP(28,5)=SGP(25,5)
GWT(1,5)=FACT*0.5079372/10.
DO 31 I=2,4
      GWT(I,5)=FACT*0.5048531/100.
31 CONTINUE
DO 32 I=5,7
      GWT(I,5)=FACT*0.2198641/10.
32 CONTINUE
DO 33 I=8,10
      GWT(I,5)=FACT*0.1088620/10.
33 CONTINUE
DO 34 I=11,13
      GWT(I,5)=FACT*0.4166142/10.
34 CONTINUE
DO 35 I=14,16
      GWT(I,5)=FACT*0.4002720/10.
35 CONTINUE
DO 36 I=17,22
      GWT(I,5)=FACT*0.4250674/100.
36 CONTINUE
DO 37 I=23,28
      GWT(I,5)=FACT*0.2370388/10.
37 CONTINUE
DO 40 IJ=6,8
      II=IJ-3
      IF (IJ.EQ.6) IK=16
      IF (IJ.EQ.7) IK=19
      IF (IJ.EQ.8) IK=28
      DO 50 IL=1,IK
          SGP(IL,IJ)=0.5*SGP(IL,II)
          TGP(IL,IJ)=0.5*TGP(IL,II)
          GWT(IL,IJ)=GWT(IL,II)/4.
50 CONTINUE
IK1=IK+1
IK2=IK*2
DO 60 IL=IK1,IK2
      JJ=IL-IK
      SGP(IL,IJ)=0.5*(1.0+SGP(JJ,II))
      TGP(IL,IJ)=0.5*TGP(JJ,II)
      GWT(IL,IJ)=GWT(JJ,II)/4.0
60 CONTINUE
IK3=IK2+1
IK4=IK2+IK
DO 70 IL=IK3,IK4
      JJ=IL-IK2
      SGP(IL,IJ)=0.5*SGP(JJ,II)
      TGP(IL,IJ)=0.5*(1.+TGP(JJ,II))
      GWT(IL,IJ)=GWT(JJ,II)/4.0
70 CONTINUE
IK5=IK4+1
IK6=IK4+IK
DO 80 IL=IK5,IK6

```

```
JJ=IL-IK4
SGP(IL,IJ)=0.5*(1.0-SGP(JJ,II))
TGP(IL,IJ)=0.5*(1.0-TGP(JJ,II))
GWT(IL,IJ)=GWT(JJ,II)/4.
80  CONTINUE
40  CONTINUE
      RETURN
      END
```

## Appendix B. FEM Session Files

Session file for BEM node/mesh generation using COSMOS/M

Session file for 1/4 pin fin (with weld fillet)  
Generates surface meshed pin fin geometry for subsequent BEM analysis  
G.A. Knorovsky, May 1997 using COSMOS/M v 1.70A

set coordinate system:

PLANE,Z,0,1,  
VIEW,1,1,1,0,

enter key points:

PT,1,4.49,0,0,  
PT,2,0,4.49,0,  
PT,3,-4.49,0,0,  
PT,4,0,-4.49,0,  
PT,5,0,0,0,

generate model edges and internal curves:

CRPCIRCLE,1,5,1,1.5875,360,4,  
SCALE,0,  
CRPLINE,5,1,2,3,4,1,  
PTGEN,1,1,5,1,0,0,0,.889,  
CRPLINE,9,10,11,12,13,10,  
CRRELOC,1,4,1,0,0,0,7.239,  
SCALE,0,  
CRGEN,1,1,4,1,0,0,0,-6.35,  
CRRELOC,13,16,1,0,0,0,1.5,  
PT,27,0,0,.889,  
CRPCIRCLE,17,14,10,2.25,360,4,  
CRLINE,21,1,10,  
CRLINE,22,4,13,  
CRLINE,23,3,12,  
CRLINE,24,2,11,  
CRLINE,25,12,29,  
CRLINE,26,11,28,  
CRLINE,27,10,27,  
CRLINE,28,13,30,  
CRLINE,29,25,29,  
CRLINE,30,24,28,  
CRLINE,31,26,30,  
CRLINE,32,23,27,  
CRLINE,33,17,25,  
CRLINE,34,16,24,  
CRLINE,35,15,23,  
CRLINE,36,18,26,  
CRLINE,37,5,1,  
CRLINE,38,5,2,  
CRLINE,39,5,3,  
CRLINE,40,5,4,

generate model surfaces:

SF3CR,1,5,38,37,0,  
SF3CR,2,6,39,38,0,  
SF3CR,3,7,40,39,0,  
SF3CR,4,8,37,40,0,  
PTGEN,1,5,5,1,0,0,0,7.239,  
SF4CR,5,24,5,21,9,0,  
SF4CR,6,24,6,23,10,0,  
SF4CR,7,23,7,22,11,0,  
SF4CR,8,21,8,22,12,0,  
SF4CR,9,9,27,17,26,0,  
SF4CR,10,10,26,18,25,0,  
SF4CR,11,11,25,19,28,0,

```
SF4CR,12,12,28,20,27,0,  
SF4CR,13,17,32,13,30,0,  
SF4CR,14,18,30,14,29,0,  
SF4CR,15,19,29,15,31,0,  
SF4CR,16,20,31,16,32,0,  
SF4CR,17,1,34,13,35,0,  
SF4CR,18,2,33,14,34,0,  
SF4CR,19,3,36,15,33,0,  
SF4CR,20,4,35,16,36,0,  
SFPTCR,21,1,31,0,  
SFPTCR,22,2,31,0,  
SFPTCR,23,3,31,0,  
SFPTCR,24,4,31,0,  
SF4PT,25,1,2,3,4,0,
```

designate element groups (common boundary conditions) and type (SHELL9 = 9 pt quadrilateral element), then mesh corresponding surfaces:

```
bottom of heat exchanger shell:  
EGROUP,1,SHELL9,0,0,0,0,0,0,0,  
M_SF,25,25,1,9,2,2,1,1,  
cut edges of hx shell:  
EGROUP,2,SHELL9,0,0,0,0,0,0,0,  
M_SF,5,8,1,9,1,2,1,1,  
top of hx shell:  
EGROUP,3,SHELL9,0,0,0,0,0,0,0,  
MA_NUSF,9,12,1,1,1,1,1,0,  
MASFCH,9,12,1,Q,9,1,3,0.4,2,5,  
cylindrical and fillet portions of pin:  
EGROUP,4,SHELL9,0,0,0,0,0,0,0,  
M_SF,13,16,1,9,2,1,1,1,  
M_SF,17,20,1,9,2,2,1,1,  
end of pin:  
EGROUP,5,SHELL9,0,0,0,0,0,0,0,  
MA_SF,21,24,1,0,4.9,0,  
MASFCH,21,24,1,Q,9,1,3,0.4,2,5,  
  
SCALE,0,  
VIEW,1,1,1,0,  
SCALE,0,
```

apply pressure loading to check for inside-out surfaces:  
PSF,5,1,25,1,1,1,4,  
VIEW,1,1,1,0,

fix those which are flipped:  
ELRELOC,57,68,1,2,0,0,14.478,180,0,0, (elements on end of pin)  
ELRELOC,9,10,1,2,-4.49,-4.49,0,0,0,180, (elements on one cut edge of shell)  
ELRELOC,7,8,1,2,-4.49,4.49,0,0,0,180, (elements on another cut edge of shell)  
VIEW,1,0,0,0,  
ELRELOC,1,4,1,1,180,0,0, (elements on bottom of shell)

merge nodes within element groups (determined by listing nodes, which includes their EG information), then renumber nodes/elements consecutively (compress)  
NMERGE,1,25,1,0.0001,1,1,0,  
NMERGE,26,85,1,0.0001,1,1,0,  
NMERGE,86,185,1,0.0001,1,1,0,  
NMERGE,186,345,1,0.0001,1,1,0,  
NMERGE,346,421,1,0.0001,1,1,0,  
NCOMPRESS,1,421,  
ECOMPRESS,1,68,

### Session file for FEM model of pin fin COSMOS/M

Session file for GEOSTAR 1.70A to generate and analyze by FEM a welded pin fin:  
G.A. Knorovsky, June, 1997

```

set orientation:
PLANE,Z,0,1,
VIEW,1,1,1,0,

enter key points:
PT,1,0,0,0,
PT,2,6.35,0,0,
PT,3,6.35,6.35,0,
PT,4,0,6.35,0,
PT,5,3.175,3.175,0,
SCALE,0,

generate edges and internal curves:
CRPCIRCLE,1,5,1,1.5875,360,4,
CRPLINE,5,1,2,3,4,1,
CRPCIRCLE,9,5,1,2.25,360,4,
CRPLINE,13,1,10,10,
CRPLINE,14,2,11,11,
CRPLINE,15,3,12,12,
CRPLINE,16,4,13,13,
CRPLINE,17,10,6,6,
CRPLINE,18,11,7,7,
CRPLINE,19,12,8,8,
CRPLINE,20,13,9,9,

generate surfaces:
SF4CR,1,5,14,9,13,0,
SF4CR,2,6,15,10,14,0,
SF4CR,3,7,16,11,15,0,
SF4CR,4,8,13,12,16,0,
SF4CR,5,9,18,1,17,0,
SF4CR,6,10,19,2,18,0,
SF4CR,7,11,20,3,19,0,
SF4CR,8,12,17,4,20,0,

define material properties for elements to be generated:
MPROP,1,KX,13.4E-3,ALPX,13.2E-6,EX,200000,NUXY,.3,C,442,DENS,8.8E-6,

generate surface elements (Default element, but these will be deleted after volume
elements are generated in a subsequent step):
M_SF,1,1,1,4,4,1,1,1,
M_SF,2,2,1,4,4,1,1,1,
M_SF,3,3,1,4,4,1,1,1,
M_SF,4,4,1,4,4,1,1,1,
M_SF,5,8,1,4,4,1,1,1,
SF4CR,9,1,2,3,4,0,
SFPTBRK,9,5,0.0001,0,
SCALE,0,
M_SF,9,12,1,4,2,2,1,1,

define volume element (8-node solid)
ACTDMESH,VL,1,
EGROUP,1,SOLID,0,1,0,0,0,0,0,
ACTSET,MP,1,

generate volume elements from surface elements previously defined (hx shell):
VLEXTR,1,12,1,Z,.889,1,-1,

define fillet as triangle, then generate 2D weld collar mesh:
PT,46,4.7625,3.175,.889,
PT,47,5.425,3.175,.889,
PT,48,4.7625,3.175,2.389,
CRPLINE,101,30,47,48,30,
SF3CR,74,101,103,102,0,
M_SF,74,74,1,4,1,2,1,1,

```

```

generate more volume elements:
ACTDMESH,PH,1,
PHEXTR,SF,41,41,1,Z,1.5,2,-1,1,0.283441,0.0001, (bottom of pin under weld fillet)
PHEXTR,SF,46,54,4,Z,1.5,2,-1,1,0.283435,0.0001,
PHEXTR,SF,75,75,1,Z,4.85,6,-1,1,0.283441,0.0001, (top of pin above weld fillet)
PHEXTR,SF,80,88,4,Z,4.85,6,-1,1,0.283435,0.0001,
CSYS,3,0,5,3,4,
ACTSET,CS,3,
PHSWEEP,SF,74,74,1,Z,360,4,4,1,1,0.6,0.0001, (generate 3D weld collar)
VIEW,0,0,1,0,
ACTSET,CS,0,
VIEW,1,1,1,0,
SCALE,0,

merge nodes, renumber nodes and elements sequentially:
NMERGE,1,NDMAX,1,.025,0,0,0,
NCOMPRESS,1,NDMAX,
ECOMPRESS,1,ELMAX,

apply isothermal temperature condition to bottom of shell:
NTSF,1,750,12,1,
ECHECK,1,256,1,5,0,

delete surface elements no longer needed:
EDELETE,1,48,1,

renumber elements:
ECOMPRESS,1,256,

apply convective boundary conditions to surfaces:
CESF,13,.0001,1627,18,5,0,
CESF,22,.0001,1627,26,4,0,
CESF,119,.0002,1627,122,1,0,
CESF,92,.0002,1627,93,1,0,
CESF,97,.0002,1627,99,2,0,
CESF,101,.0002,1627,102,1,0,
CESF,105,.0002,1627,106,1,0,

set analysis type and defaults for iteration, tolerances, data to be saved, etc.:
A_THERMAL,S,0.001,1,1,20,0,
HT_OUTPUT,1,1,1,

run steady-state thermal analysis
C* R_THERMAL,

```

## Appendix C. Conversion Code

CONVERT.CPP, the main program that controls the conversion process.

```
*****
#include <fstream.h>
#include "model.h"
#include "node.h"
void packet1(const model & nl, ostream & fout);

void main(){
    model md;

    char filein[25]={0}, fileout[25]={0};
    cout<<"Enter the filename from Cosmos listlog "<<flush;
    cin>>filein;
    cout<<"Enter the filename for BE input deck "<<flush;
    cin>>fileout;

    ifstream fin(filein);                                //Input
    ofstream fout(fileout);                             //Output

    fin>>md;

    md.applybc(); //apply element-based bc's to nodes

    md.scandir(); //check directions

    char yn='y';
    double nx,ny,nz;
    cerr<<"Would you like to check with a different center? (y/n) "<<flush;
    cin>>yn;
    while (yn!='n' && yn!='N'){
        cerr<<"Enter a new center as x y z: "<<flush;
        cin>>nx,ny,nz;
        md.scandir(nx,ny,nz);
        cerr<<"Would you like to check with a different center? (y/n) "<<flush;
        cin>>yn;
    }

    //Print out packet 1
    packet1(md,fout);

    //Print out packet 2: nodes w/ bc's      & packet 3: element list
    fout<<md;

    //No packet 4, IEXTRA=0
    //Print packet 5, collocation points
    fout<<"Replace this line with # of collocation points"<<endl;
    fout<<"X Y Z Replace and duplicate this line for # of collocation
points"<<endl;

}

void packet1(const model & md, ostream & fout){
    fout<<"Single Pin Fin Thermal Model"<<endl;
    fout<<"Generated by Cosmos and converted to Ingber input deck"<<endl;
    fout<<"More Title Here"<<endl;
    fout<<"0 0 "<<endl;
    int nn=md.nnodes();
    int ne=md.nel();
    fout<<nn<<' '<<ne<<endl;
}
```

The model class contains the elements and nodes that make up the model

\*\*\*\*\*

```
#ifndef MODEL_H
#define MODEL_H
#include <fstream.h>
#include <assert.h>
#include <string.h>

#include "node.h"
#include "element.h"

class model{
private:
    node center;

    void addsize1(int n=100);
    int size;
    int numels;
    element * elements;

    void addnsize(int n=100);
    node * nodes;
    int sizen;
    int numnodes;

public:
    model(int elements=100, int nodes=100);
    ~model();

    int nel() const;
    int nnodes() const;
    friend ostream & operator << (ostream & fout, const model & md);
    friend istream & operator >> (istream & fin, model & md);

    void applybc();
    void scaneg(int neg, int eg[] ) const;
    void geteg(int nodeg[]) const;

    void scandir(double nx=-999, double ny=-999, double nz=-999);
    double dir(const element & e);

};

#endif
```

Model Class Implementation:

\*\*\*\*\*

```
#include "model.h"
```

```
model::model(int e,int n)
{
    size=e;
    numels=0;
    elements=new element[e];
    sizen=n;
    numnodes=0;
    nodes=new node[n];
    node center;
```

```
}
```

```
model::~model()
```

```

{
    delete [] elements;
    delete [] nodes;
}

void model::addsize1(int n)
{
    element * larger_array;
    larger_array=new element[size+n];
    for (int i=0;i<numels;i++){
        larger_array[i]=elements[i];
    }
    delete [] elements;
    elements=larger_array;
    size += n;
}

void model::addnsize(int n)
{
    node * larger_array;
    larger_array=new node[sizen+n];
    for (int i=0;i<numnodes;i++){
        larger_array[i]=nodes[i];
    }
    delete [] nodes;
    nodes=larger_array;
    sizen += n;
}

istream & operator >> (istream & fin, model & md)
{
    //Read in and discard heading line, Node list is first
    fin.clear();
    char line[100];
    char ready[]="Z-C";
    do{
        fin.getline(line,80);
        cout<<"Node header discard:<<endl<<line<<endl;
    }
    while( ! strstr(line,ready));

    //Read in nodes until a failure occurs, indicating element header read:
    //for(int i=nl.numnodes;i<nl.sizen && fin>>nl.nodes[i];i++){
    for(int i=md.numnodes;fin>>md.nodes[i];i++){
        //If numnodes = sizen, then we may have more, so add to sizen
        //Note we ignore case of an even 100's of nodes, so array could
        //inadvertantly get too big, but who cares!
        md.numnodes++;
        if (md.numnodes==md.sizen-1){
            md.addnsize();
        }
        md.center += md.nodes[i]; //sum nodes to find center for surface
    }
    check
    }
    md.center/=md.numnodes; //average location to find center

    //Read in and discard heading line for elements
    fin.clear();
    fin.getline(line,80);
    cout<<"Element header discard:<<endl<<line<<endl;

    //Read in elements until a failure occurs, indicating eof:
    //for(int i=ell.numels;i<ell.size && fin>>ell.elements[i] && !fin.eof();i++){
    for(i=md.numels;fin>>md.elements[i] && !fin.eof();i++){
        //If numnodes = size, then we may have more, so add to size
    }
}

```

```

        //Note we ignore case of an even 100's of nodes, so array could
        //inadvertantly get too big, but who cares!
        md.numels++;
        //cerr<<ell.numels<< ' '<<ell.size<< ' '<<i<<endl;
        if (md.numels==md.size-1){
            md.addsize1();
        }
    }
    return fin;
}

ostream & operator << (ostream & fout, const model & md)
{
    //Print packet 2, the nodes
    for (int i=0;i<md.numnodes;i++){
        fout<<md.nodes[i]<<endl;

    }
    //Print packet 3, the elements
    for (i=0;i<md.numels;i++){
        fout<<md.elements[i]<<endl;
    }
    return fout;
}

int model::nel() const
{
    return numels;
}

int model::nnodes() const
{
    return numnodes;
}

void model::applybc()
{
    //This routine applies the boundary conditions found in el to the nodes
    const int maxbcs=10;
    int eg[maxbcs]={0};           //Element group, specifies bc's
    int neg=0;
    int nbdy[maxbcs];
    int i;
    double par1[maxbcs];
    double par2[maxbcs]={0.0};

    //First we determin how many element groups there are
    scaneg(maxbcs,eg);

    //Now we get the parameters for each element group:
    cout<<"Boundary conditions:<<endl;
    cout<<"NBDY=1: PAR1=specified T, PAR2=0 "<<endl;
    cout<<"NBDY=2: PAR1=specified Flux, PAR2=0 "<<endl;
    cout<<"NBDY=3: PAR1=1/h, PAR2= T inf "<<endl;

    for(i=0;i<maxbcs;i++){
        if (eg[i] != 0){
            cout<<"For element group "<<eg[i]<<" enter NBDY, PAR1, PAR2: "<<flush;
            cin>>nbdy[i]>>par1[i]>>par2[i];
        }
    }

    //Now we scan elements and apply BC to each node
    //Array bcapplied is used to look for conflicting bc's applied to same node
    int *bcapplied;
    bcapplied=new int [numnodes];
}

```

```

        for( i=0;i<numnodes;i++){
            bcapplied[i]=0;
        }

        geteg(bcapplied);

        //Now we apply the list of BC's to the nodes
        for(i=0;i<numnodes;i++){
            nodes[i].bc(nbdf[bcapplied[i]],par1[bcapplied[i]],par2[bcapplied[i]]);
        }
    }

void model::scaneg(int neg, int eg[] ) const
{
    //First we determin how many element groups there are
    for ( int i=0;i<numels;i++){
        assert(elements[i].eg() < neg);
        eg[elements[i].eg()]=elements[i].eg();
    }
}

void model::geteg(int nodeg[]) const
{
    int nlist[9];
    for(int i=0;i<numels;i++){
        elements[i].tellnodes(nlist);
        for(int j=0;j<9;j++){
            if(nodeg[nlist[j]] != 0 && nodeg[nlist[j]] != elements[i].eg()){
                cerr<<"Conflicting BC: node "<<nlist[j]+1<<" was eg#"
"<<nodeg[nlist[j]]<<, requested "<<elements[i].eg()<<" on element "<<i+1<<endl;
            }else{
                nodeg[nlist[j]]=elements[i].eg();
            }
        }
    }
}

void model::scandir(double nx, double ny, double nz)
{
    if (nx != -999){
        center=node(nx,ny,nz);
    }
    for ( int i=0;i<numels;i++){
        if(dir(elements[i])<0){
            cout<<"Possible orientation problem, element
"<<i+1<<endl<<elements[i]<<endl;
        }
    }
    cout<<"center was at "<<center.getx()<<' '<<center.gety()<<' '<<center.getz()<<endl;
}

double model::dir(const element & e)
{//Return the relative direction of the normal and the vector from the center
 //Negative could indicate the element is bass backwards

    //Check element normal direction against center of nodal mass
    double nx=0,ny=0,nz=0,cx=0,cy=0,cz=0;
    double ax,ay,az,bx,by,bz,dp;
    int nlist[9];

    e.tellnodes(nlist);

    //Vector from center to 2nd node
    cx=nodes[nlist[1]].getx()-center.getx();
    cy=nodes[nlist[1]].gety()-center.gety();
    cz=nodes[nlist[1]].getz()-center.getz();
}

```

```

//Vector normal to second node
ax=nodes[nlist[1]].getx()-nodes[nlist[0]].getx();
ay=nodes[nlist[1]].gety()-nodes[nlist[0]].gety();
az=nodes[nlist[1]].getz()-nodes[nlist[0]].getz();
bx=nodes[nlist[2]].getx()-nodes[nlist[1]].getx();
by=nodes[nlist[2]].gety()-nodes[nlist[1]].gety();
bz=nodes[nlist[2]].getz()-nodes[nlist[1]].getz();
nx=ay*bz-az*by;
ny=az*bx-ax*bz;
nz=ax*by-ay*bx;
//Dot product to check relative direction
dp=cx*nx+cy*ny+cz*nz;
return dp;
}

```

The node class defines the node abstract data type:

```

*****
#ifndef NODE_H
#define NODE_H
#include <fstream.h>

class node{
private:
    int nbdf;
    double par2;
    double par1;
    double z;
    double y;
    double x;
    int globalnum;
public:
    void bc(int btype,double p1,double p2);
    friend ostream & operator << (ostream & fout, const node & nd);
    friend istream & operator >> (istream & fin, node & nd);
    node(double nx=0,double y=0, double z=0);
    void operator += (const node & n);
    void operator /= (const double & n);
    double getx();
    double gety();
    double getz();
};
#endif

#include "node.h"

node::node(double nx, double ny, double nz)
{
    x=nx;
    y=ny;
    z=nz;
    globalnum=nbdf=0;
    par1=par2=0.0;
}

void node::operator += (const node & n)
{//Overloads the += operator to sum nodal locations
    x+=n.x;
    y+=n.y;
    z+=n.z;
}

```

```

}

void node::operator /= (const double & n)
{ //Overlaods the += operator to summ nodal locations
    x/=n;
    y/=n;
    z/=n;
}

double node::getx()
{return x; }

double node::gety()
{return y; }

double node::getz()
{return z; }

istream & operator >> (istream & fin, node & nd)

{ //Reads the current node from the file created by Cosmos.
    //Assumes format is from nlist, sent to file by listlog
    fin>>nd.globalnum;
    fin>>nd.x>>nd.y>>nd.z;
    return fin;
}

ostream & operator << (ostream & fout, const node & nd)

{ //This returns a node card for NPOT3D, a BEM code by Ingber
    //Card Packet 2
    char c=',';
    fout<<nd.globalnum<<c<<nd.x<<c<<nd.y<<c<<nd.z<<c<<nd.par1<<c<<nd.par2<<c<<nd.nbd
y<<c<<'0';
    return fout;
}

void node::bc(int btype,double p1,double p2=0)

{
    nbdy=btype;
    par1=p1;
    par2=p2;
}

```

The Element class defines the abstract data type of Element:

\*\*\*\*\*

```

#ifndef ELEMENT_H
#define ELEMENT_H

#include <fstream.h>
#include "node.h"

class element{
private:
    int elgrp;
    int node[9];

```

```

int ieltype;
int elnum;

public:
    friend ostream & operator << (ostream & fout, element el);
    friend istream & operator >> (istream & fin, element & el);
    void tellnodes(int nlist[]) const;
    int eg() const;
    element();
};

#endif

#include "element.h"

element::element()
{//Default constructor

    elgrp=0;
    ieltype=40; //40 is a quadrilateral 9-node element
}

int element::eg() const
{//Report the element's group, used for bc separation

    return elgrp;
}

void element::tellnodes(int nlist[]) const
{//report the node list for an element
    for(int i=0;i<9;i++){
        nlist[i]=node[i]-1;
    }
}

istream & operator >> (istream & fin, element & el)
{
    int garbage;
    fin>>el.elnum>>el.elgrp>>garbage>>garbage>>garbage;
    for(int i=0;i<9;i++){
        fin>>el.node[i];
    }
    return fin;
}

ostream & operator << (ostream & fout, element el)
{
    char c=',';

```

```
    fout<<el.elnum<<c<<el.ieltype;
    for (int i=0;i<9;i++){
        fout<<c<<el.node[i];
    }

    return fout;
}
```

## Distribution

### Internal (Sandia) Distribution:

<u>Mail Stop</u>	<u>Name</u>	<u>Department</u>	<u>Quantity</u>
0703	C.E. Andraka	6216	5
0703	J.B. Moreno	6216	2
0703	C.E. Tyner	6216	1
0703	T.A. Moss	6216	1
0703	R.B. Diver	6216	1
1127	K.S. Rawlinson	6215	2
1127	J.M. Chavez	6215	1
1127	Library	6215	5
0835	D.R. Adkins	9113	1
1110	R. Allen	9205	1
1405	C. A. Drewien	1822	5
0340	G. Knorovsky	1833	5
0619	Review and Approval for DOE/OSTI	12690	2
9018	Central Technical Files	8940-2	1
0899	Technical Library	4916	2

### External Distribution:

National Renewable Energy Laboratory 1

Attn: Mark Bohn (2 copies)

1617 Cole Blvd.

Golden CO 80401-3393

Brian Smith 1

University of New Mexico

Department of Computer Science

Albuquerque, NM 87131

Mark Ingber 2

University of New Mexico

Department of Mechanical Engineering

Albuquerque, NM 87131

M98004181



Report Number (14) SAND--98-0306

Publ. Date (11)

199802

Sponsor Code (18)

DOE/EE, XF

UC Category (19)

UC-1302, DOE/ER

**DOE**